METALLURGICAL EVALUATION OF DOT-3AL-2015 CYLINDER T-57003

Prepared for

U.S. Department of Transportation
400 Seventh Street S.W.
Washington, DC 20590

Prepared by:

Timothy R. Smith, Ph.D., P.E
Robin B. Michnick, Ph.D.
310 Montgomery Street
Alexandria, VA 22314

November 1998

Purchase Order No.: DTRS56-98-70066
Project No.: DC18128.000
Report No.: DC18128.000 A0F0 10/98 1001

EX.

TABLE OF CONTENTS

LIST OF FIGURES

1 Introduction

The U.S. Department of Transportation (DOT) contracted with Exponent Failure Analysis Associates (FaAA) to perform a metallurgical examination of the remains of a failed aluminum SCBA cylinder. The cylinder is a DOT-SP6498-22-1 type with serial number T57003 manufactured by Luxfer USA and incorporated into a SCOTT air pack for fire fighting use. The U.S. DOT seized the cylinder on September 9, 1997 in Allegan City, MI.

The scope of this investigation was to perform a detailed evaluation of the cylinder remains including photodocumentation and non-destructive examinations, chemical and mechanical property determination, metallographic sectioning, and fractography. The detailed work scope for this evaluation is provided in Appendix A. This report presents the findings of this evaluation.

2 Visual Examination

A visual examination of the cylinder remains was performed. The remains are shown in Figures 1 and 2 in the as-received condition. The cylinder broke apart into two large pieces. The bottom of the cylinder erupted as seen in Figure 2.

The first hydrostatic test on the cylinder was performed in 4/75, based on stampings on the neck. This is taken as its date of manufacture. Inspection stampings indicated that the cylinder had been hydrostatically re-tested in 6/83, 10/88 and 1/94. The SP6498 stampings on the neck indicate Luxfer was the manufacturer[1]. The bottom of the cylinder had stamping that indicated the heat number T358 and the cast number I-211A. A complete photodocumentation of the pieces was undertaken and is presented in Appendix B.

The fracture surfaces of the cylinder were inclined (i.e., non-radial with respect to the cylinder axis) shear-type except for a portion of the neck where the fracture surfaces were flat and radial with respect to the axis of the cylinder. In the neck region, the fracture appears to pass through a diameter of the inlet. Figure 3 shows the erupted bottom. Regions of the bottom separated from the sidewall with a crack extending into the side parallel to the axis of the cylinder. In the neck region, the inside wall of the cylinder in this region shows multiple folds (or cusps) from the original manufacturing process, Figure 4. The fracture surface on both sides of the inlet hole appears to pass through folds of this type. A slight amount of aluminum corrosion product was present on the threaded region.

[1] SP6498 is a special permit granted to Luxfer, USA Ltd. to manufacture, mark and sell cylinders for the use in transportation in commerce involving certain liquefied and nonliquefied compressed gases. Luxfer was later granted the E6498 exemption (07/76) to the provisions of DOT's then applicable Hazardous Materials Regulations for the same purpose as the special permit. The special permit and exemption satisfy the DOT-3AL section of 49 CFR-178.45.

3 Quantitative Chemical Analysis

Samples of chips, taken using an electric drill from the neck, the sidewall, and the bottom of the cylinder, were dissolved in solution and analyzed by atomic absorption spectrometry to determine their chemical composition. The results of this analysis are shown in Table 1 and indicate that the cylinder conforms to the Aluminum Association (AA) 6351 alloy specification and satisfies the DOT-3AL specification for aluminum alloy chemistry.

Table 1: Chemistry of the Cylinder

	Composition (wt.%)				
Element	Test Result Neck	Test Result Sidewall	Test Result Bottom	49 CFR-178.46-5 Specification (low)	49 CFR-178.46-5 Specification (high)
Mg	0.65	0.65	0.66	0.40	0.80
Si	1.06	1.05	1.07	0.70	1.30
Ti	0.02	0.02	0.02	0.00	0.20
Mn	0.60	0.59	0.61	0.40	0.80
Fe	0.27	0.29	0.28	0.00	0.50
Cu	0.04	0.03	0.04	0.00	0.10
Zn	<0.01	<0.01	<0.01	0.00	0.20
Bi	<0.005	<0.005	<0.005	0.00	0.01
Pb	<0.005	<0.005	<0.005	0.00	0.01
Al	balance	balance	balance	balance	balance

Chemical composition determined by atomic absorption spectrometry in accordance with the ASTM-E663 and ASTM-D3335 standards.

These results show compliance with both the DOT exemption E6498 and the current DOT federal regulation 49 CFR-178.46-5 with no significant variations based on the sample location from within the cylinder. Note that the Pb levels found were below the detection threshold of 50 weight-ppm (6.5 atomic-ppm[2]) for the sample size provided for chemical testing. In addition, the Bi-levels were below 50 weight-ppm (6.5 atomic-ppm)

4 Mechanical Testing

4.1 Tensile Testing

Full thickness tensile test coupons from the cylinder wall, aligned along the cylinder axis, were tested at room temperature in accordance with ASTM B557 and following the procedure given by 49 CFR 178.46-13. The samples were machined from the segment marked "Mech" in Figure 5. The results of these tests are shown in Table 2.

[2] Calculated the equation: atomic-ppm (Pb) = weight-ppm (Pb)*GMW(Al)/GMW(Pb); where GMW is the gram molecular weight of the element in parenthesis. The same equation was used for the bismuth level with Bi replacing Pb.

The measured average strength values are well above the requirements of E6498 and exceed the current 49 CFR 178.46-5 minimum specification. The test results also meet the elongation requirements. They compare well with values of 42.8 ksi yield strength, 49.3 ksi ultimate strength, and 13% elongation (2 inch gauge length), published for AA6351 in T6 temper [1]. The DOT E6498 requires that the material be AA6351-T6.

Table 2: Mechanical Properties

Test	Yield (ksi)	UTS (ksi)	Elongation (%)	49 CFR 178.46-5 Yield (min.) (ksi)	49 CFR 178.46-5 UTS (min.) (ksi)	49 CFR 178.46-5 Elongation (min.) (%)
T03-01	46.2	51.5	15.4	37.0	42.0	14
T03-02	47.0	51.8	17.3	37.0	42.0	14
T03-03	47.3	51.4	15.6	37.0	42.0	14

Notes:

1. Tests were performed in accordance with the ASTM B 557 standard and following the procedure given by 49 CFR 178.46-13; gauge length was 2 inches.
2. Yield denotes the yield strength (0.2% offset), UTS denotes ultimate tensile strength.
3. Elongation values from the flat coupons tested here differ from the 49 CFR 178.46-5 values based on cylindrical specimens.

4.2 Hardness Testing

Rockwell hardness measurements were made on a slice removed from the tank sidewall area. A total of five measurements were taken using a Leco RT-370 Rockwell hardness tester with a 100-kg load; the results are shown in Table 3.

Table 3: Hardness Measurements

Component	Indent No.	Hardness (Rockwell B)	Average Hardness (Rockwell B)
2A-5A	1	61.1	61.7
	2	61.0	
	3	62.2	
	4	62.1	
	5	62.3	

5 Sectioning and Metallography

The sections cut from cylinder fragment 2A-1 are shown in Figure 7. Sections of the fracture surface on both sides of the inlet were cut such that the flat-faced portion of the fracture surface was separated from the fragment. Two wafers were generated in the process.

A section in the neck region of sample 2A-1 was sliced (2A-1A) and then polished and etched to reveal its microstructure, Figure 8. Note that the grain size varies from relatively large to small, compared to the thickness at the neck. Also note the directionality of the grains and their relative sizes along the neck and the commencement of the cylinder body. This grain configuration is a consequence of the neck forming process used during manufacturing. Figures 9, 10, and 11 show regions A, B, and C at higher magnifications. Small cracks are seen within these areas. Some of the cracks have origins at the surface while others do not. The cracks show fine-scale branches and appear to be discontinuous.

A minor amount of corrosion pitting and smearing or galling of the aluminum , threads is visible in Figure 10. Figure 12 shows energy dispersive spectra (EDS) taken from at or near the corrosion pits of the threaded region of sample 2A-2. Note the O, Ca, Cl, Fe, and Cu peaks, all of which are corrosion product or contaminants. The Cu and Fe are most probably from the treaded end of the regulator assembly that was screwed into the inlet hole during service.

6 Fractography

The wafer (samples 2A-1 and 2A-2) containing the flat-face fracture surface is shown in Figure 6. Optical examination revealed that the flat-face region of the fracture surface shows little macroscopic ductility. Just outside of this region, the fracture surface transitioned to an inclined shear-type of fracture.

Section 2A-2 was examined optically and in the scanning electron microscope (SEM). The region just below the inlet hole threads and close to the inside of the cylinder contained some coating[3] used to line the cylinder, suggesting that a deep fold was present at this location at the time of manufacture. Figure 13 shows a series of SEM fractographs taken from this fracture surface.

Region 1 is at the inside surface close to the inlet hole threads. This region shows intergranular fracture with fine poorly formed dimpling on the grain facets. In the area of the threads, region 2, similar features are seen. Region 3 is similar as well with an increase in the extent of dimpling. Region 4 marks a transition with part of the area showing a mixture of intergranular and transgranular fracture with the remaining area indicative of ductile, dimpled rupture. Region 5 shows predominantly ductile dimpled rupture with a minor amount intergranular faceting (with microdimpling on these facets) as a failure mode. This is the predominant failure mode for the remainder of the neck region.

SEM fractographs of the fracture surface from one of the tensile specimens (T2A) used for mechanical property determination are shown in Figure 14. Note that the fracture surface is ductile dimpled rupture. This morphology is consistent with fractographic studies of similar Al alloys in tensile and toughness testing [2]. This morphology compares well with the dimpled rupture morphologies shown in Figure 13.

[3] EDS analysis of this coating (not shown) had Al and O peaks, indicating that the coating is Al-based perhaps formed by anodizing the cylinder interior.

7 Discussion

Examination and testing of the cylinder remains demonstrates that the subject cylinder meets the chemical and mechanical property requirements of DOT E6498 specifications and in the current DOT 49 CFR 178.46. Both lead (Pb) and bismuth (Bi) are below the regulation limits specified in both E6498 and 49 CFR 178.46-5. The cylinder alloy complies with the Aluminum Association specification for AA6351-T6 in accordance with DOT E6498. The microstructure appears to be typical for this alloy and heat treatment.

Examination of the fracture surfaces of each cylinder fragment suggests that the failure originated from the neck region of the cylinder near to the inlet hole. The flat-faced (i.e., radial) nature of the fracture surface at the neck region, followed by a transition to an inclined (i.e., non-radial) shear type of fracture on both sides of the cylinder, suggests fast fracture initiating nearly simultaneously on diametrically opposed sides of the inlet hole, prior to final rupture. Based on Figures 9, 10, and 11, subcritical cracking clearly existed to a small extent near to the inlet hole at folds in the inside wall. The origin of the rupture is at two of these small cracks; however, the similarity in the grain sizes (Figure 8) and the failure surfaces in Regions 1-3 suggests a "tearing-out" of the grains during a rapid ductile failure outward from the small cracks. This tearing of grains and the absence of beachmarks along the fracture surface suggests that the crack growth from these initial origin areas occurred during a single event. This event is consistent with an internal pressure well in excess of normal operation (i.e., an overpressurization) of the cylinder.

Sectioning of the cylinder wall just below the threads at the inlet hole revealed multiple cracks from multiple origins at folds (or cusps) in the inside wall. These cracks are similar to the small fracture origin cracks noted above. These branched cracks are consistent with cracks found in the neck region of other DOT-6498, DOT-3AL, and DOT-7235 aluminum cylinders [3]. Since no fatigue striations or evidence of another sub-critical crack growth mechanism were found, the observed cracks are more consistent with studies of "sustained-load cracking" reported in the literature for similar Al alloys, [2, 4-8] than fatigue or another sub-critical crack growth mechanism.

8 Summary and Conclusions

A metallurgical examination of an aluminum cylinder DOT-SP6498-22-1 type with serial number T57003 showed the following results.

- This 1975-vintage cylinder meets the chemical requirements of the E6498 exemption and current 49 CFR 178.46-5 for AA6351 alloy, including lead (Pb) and bismuth (Bi) levels.
- This 1975-vintage cylinder meets the mechanical property requirements of the E6498 exemption and the current 49 CFR 178.46-5.
- Over 95% of the fracture area was a result of rapid crack propagation.
- Multiple subcritical cracks were found originating at folds in the interior wall in the neck region near the inlet hold. These folds were associated with the manufacture of the cylinder.
- Cracks showed a multiple-branched morphology; crack tips appear to be discontinuous.
- The cylinder failed when two small diametrally-opposed cracks at folds in the neck region became of critical size due to an internal pressure well above normal operation (i.e., overpressurization).
- The apparent origin of the fracture is consistent with sustained-load cracks reported in the literature for similar Al alloys.

9 References

1. J. E. Hatch, Ed., (1984), Aluminum: Properties and Physical Metallurgy, American Society for Metals, Metals Park, OH, p. 363.
2. M. Guttmann, B. Quantin, and Ph. Dumoulin, (1983), "Intergranular Creep Embrittlement by Non-soluble Impurity: Pb Precipitation Hardened Al-Mg-Si Alloys," Metal Sci., Vol. 17, No. 3, pp. 123-140.
3. J.H. Smith, (1987), "Evaluation of Cracking in Aluminum Cylinders," NBSIR 86-3492, Institute for Materials Science and Engineering, National Bureau of Standards (NBS), U.S. Dept. of Commerce, Gaithersburg, MD.
4. J.J. Lewandowski, Y.S. Kim, and N.J.H. Holroyd, (1992), "Lead-Induced Solid Metal Embrittlement of an Excess Silicon Al-Mg-Si Alloy at Temperatures of –4°C to 80°C," Met. Trans. A., Vol. 23A, pp. 1679-1689.
5. Y.S. Kim, N.J.H. Holroyd, and J.J. Lewandowski, (1989), "Pb-Induced Solid-Metal Embrittlement of Al-Mg-Si Alloy at Ambient Temperatures," *Proc. Environment-Induced Cracking of Metals*, National Association of Corrosion Engineers (NACE), pp. 371-377.
6. J.J. Lewandowski, V. Kohler, and N.J.H. Holroyd, (1987), "Effects of Lead on the Sustained-Load Cracking of Al-Mg-Si Alloys at Ambient Temperatures, " Mat. Sci & Eng., Vol. 96, pp. 185-195.
7. H.L. Stark and R.N. Ibrahim, (1992), "Crack Propagation in Aluminum Gas Cylinder Neck Material at Constant Load and Room Temperature," Eng. Fracture Mechanics, Vol. 41, No. 4, pp. 569-575.
8. H.L Stark and R.N. Ibrahim, (1988), "Crack Propagation at Constant Load and Room Temperature in an Extruded Aluminum," Eng. Fracture Mechanics, Vol. 30, No. 3, pp. 409-414.

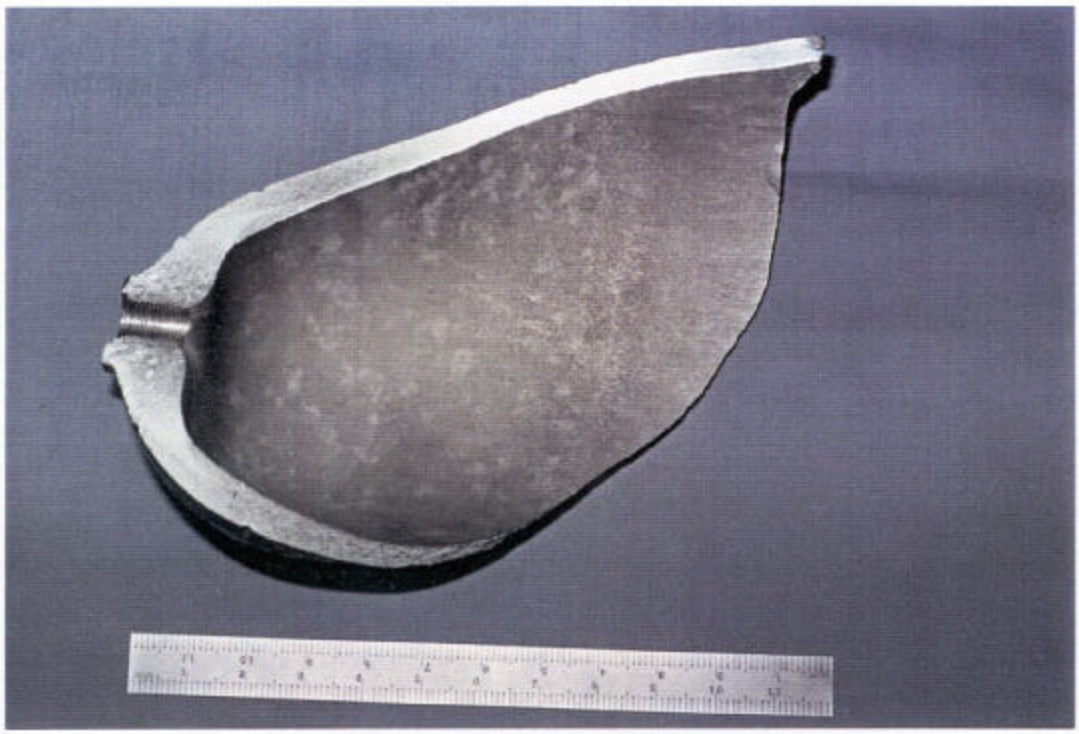

Figure 1: Cylinder remains, as-received
Fragment 2A-1. Photo ID: DC18128-R1E17

Figure 2: Cylinder remains, as-received
Fragment 1A-1. Photo ID: DC18128-R1E20

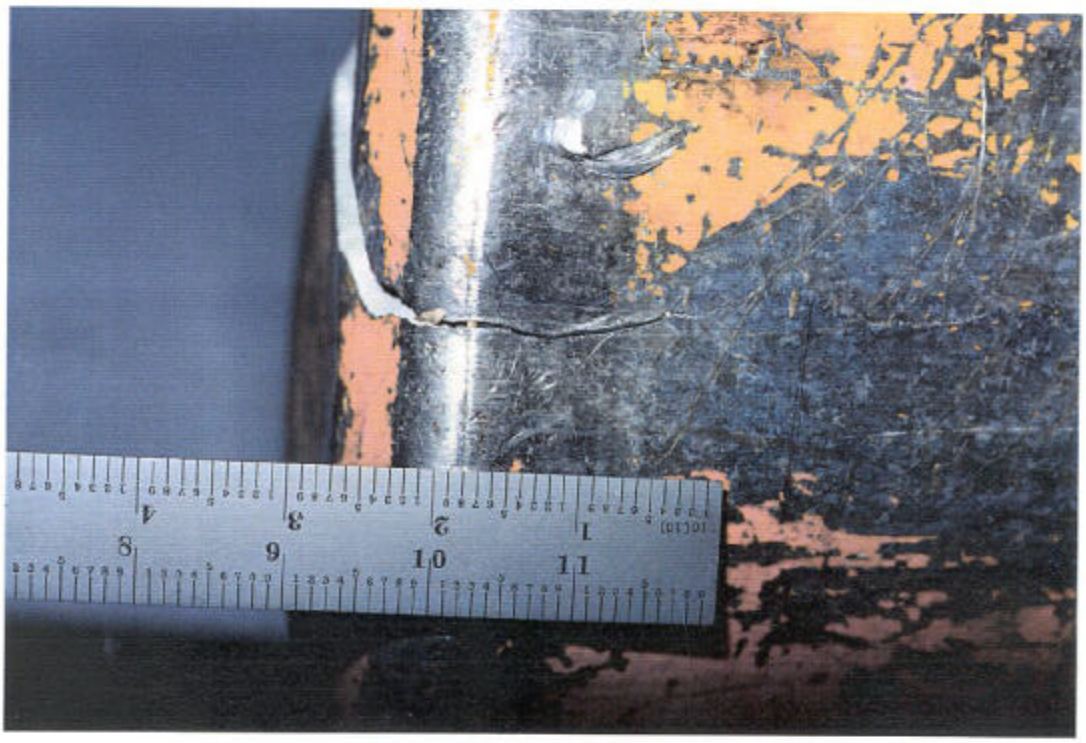

Figure 3: Cylinder remains, as-received
Fragment 1A-1. Photo ID: DC18128-R1E24

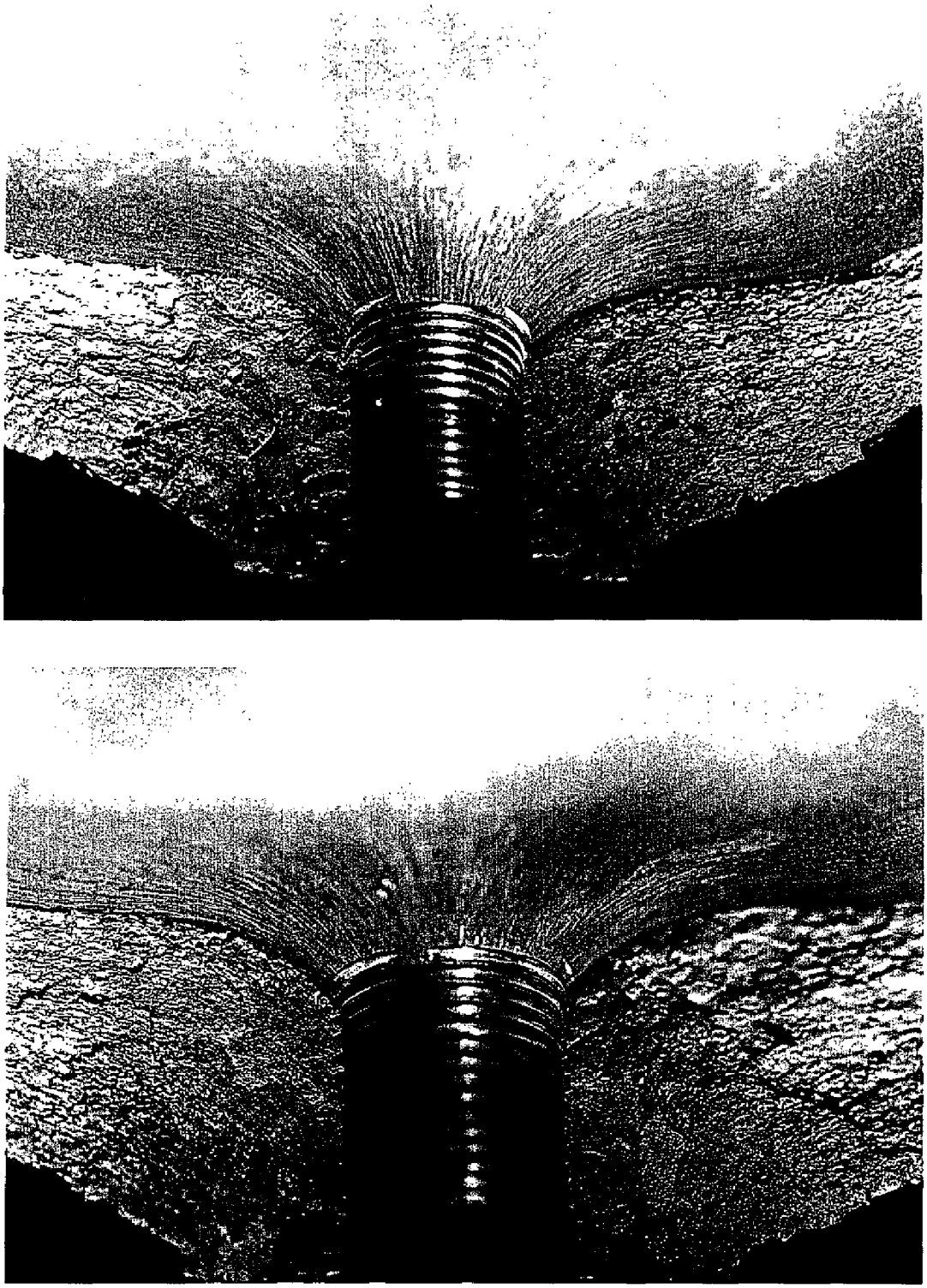

Figure 4: Fracture surface at the inlet hole.
Photo ID: DC18128-R1E9, R2E7

Figure 5: Cylinder fragments 1A-1.
(a) Sections cut. Photo ID: DC18128-R4E5.
Note "MECH" denotes the piece used for machining tensile test coupon.
(b) Tensile test coupons, DC18128-R5E11.

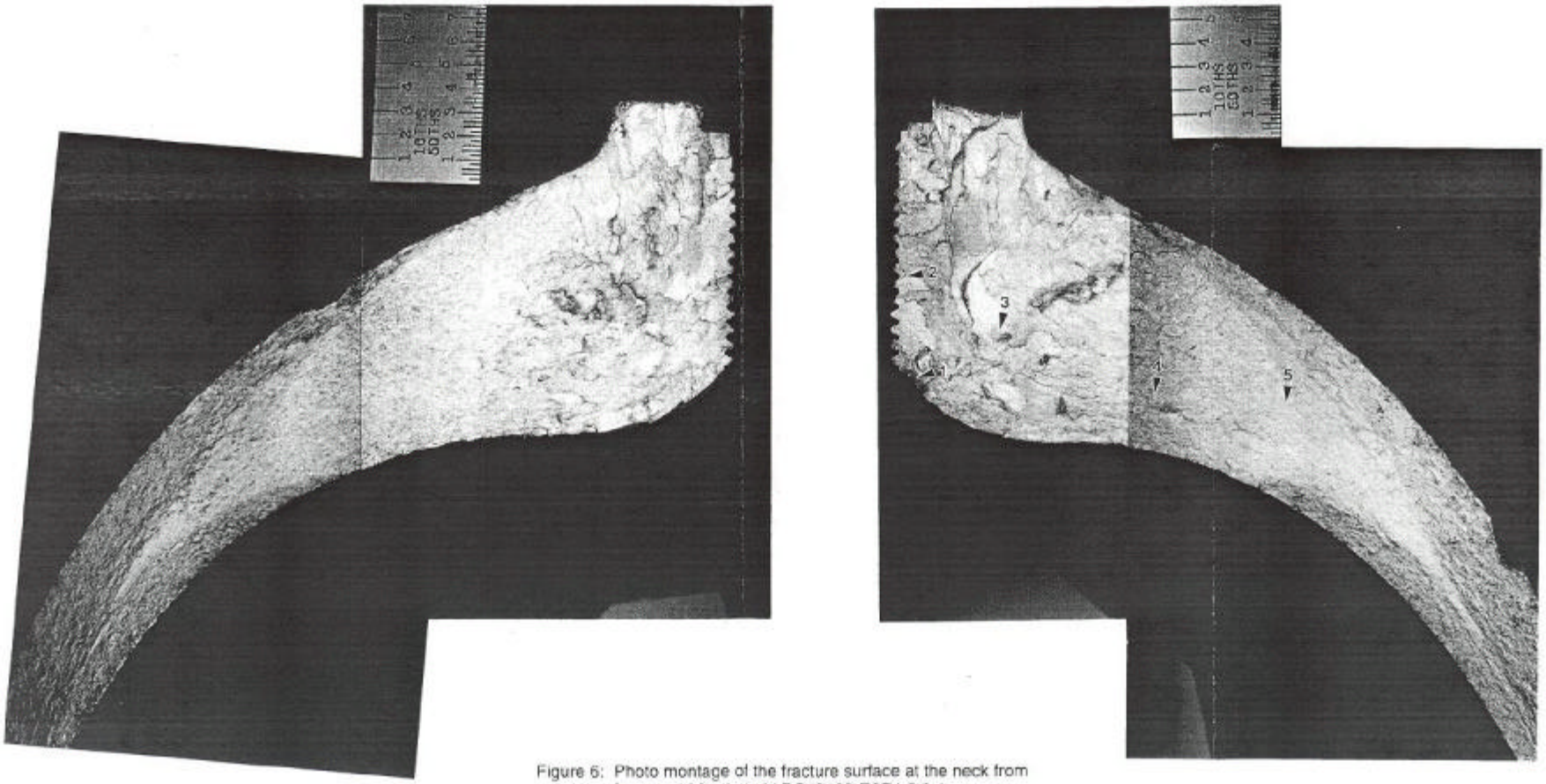

Figure 6: Photo montage of the fracture surface at the neck from fragment 2A. photo id DC18128-R3E1,2,3,4
Regions 1 through 5 represent areas for further study.

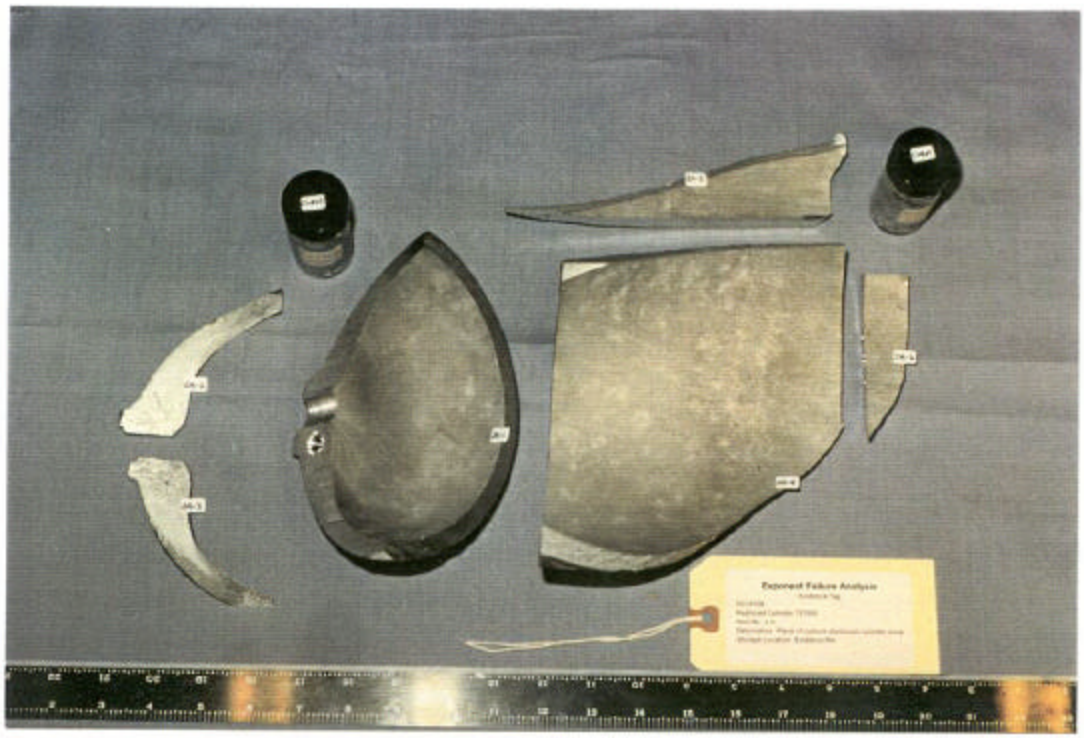

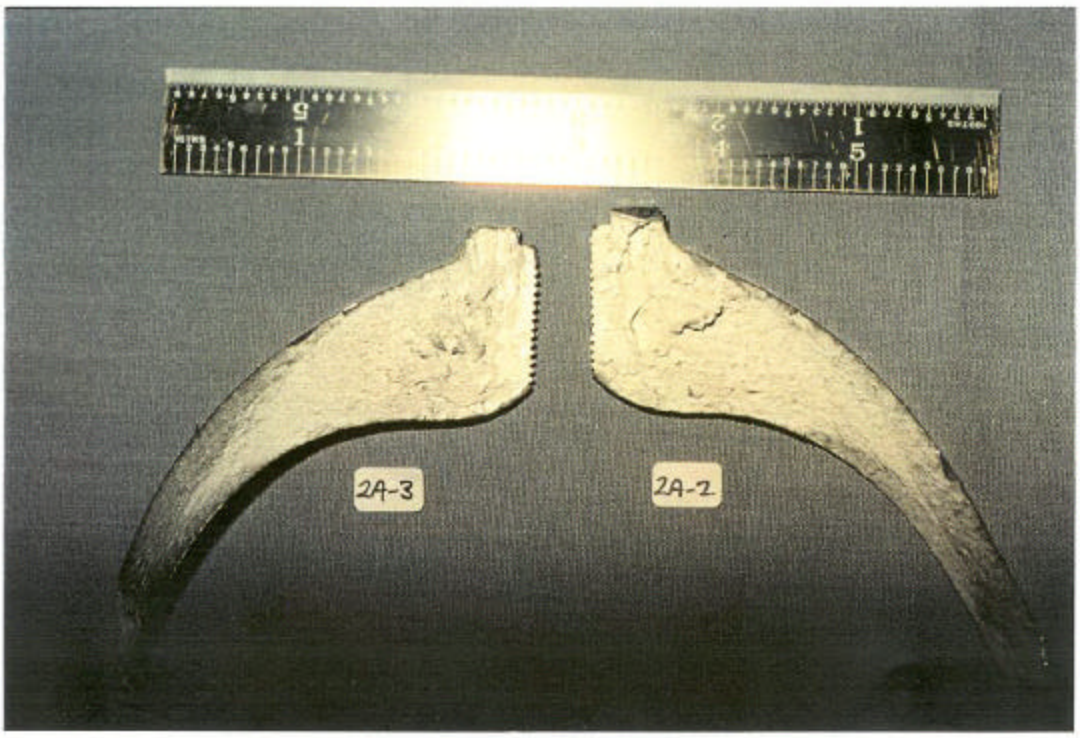

Figure 7: Sectioning of fragment 2A
(a) Overall view. Photo ID: DC18128-R3E2
(b) Close up of neck region. Photo ID: DC18128-R3E11
Note: the fracture surface portions that were removed and the drilling taken to determine chemical composition.

Ex.

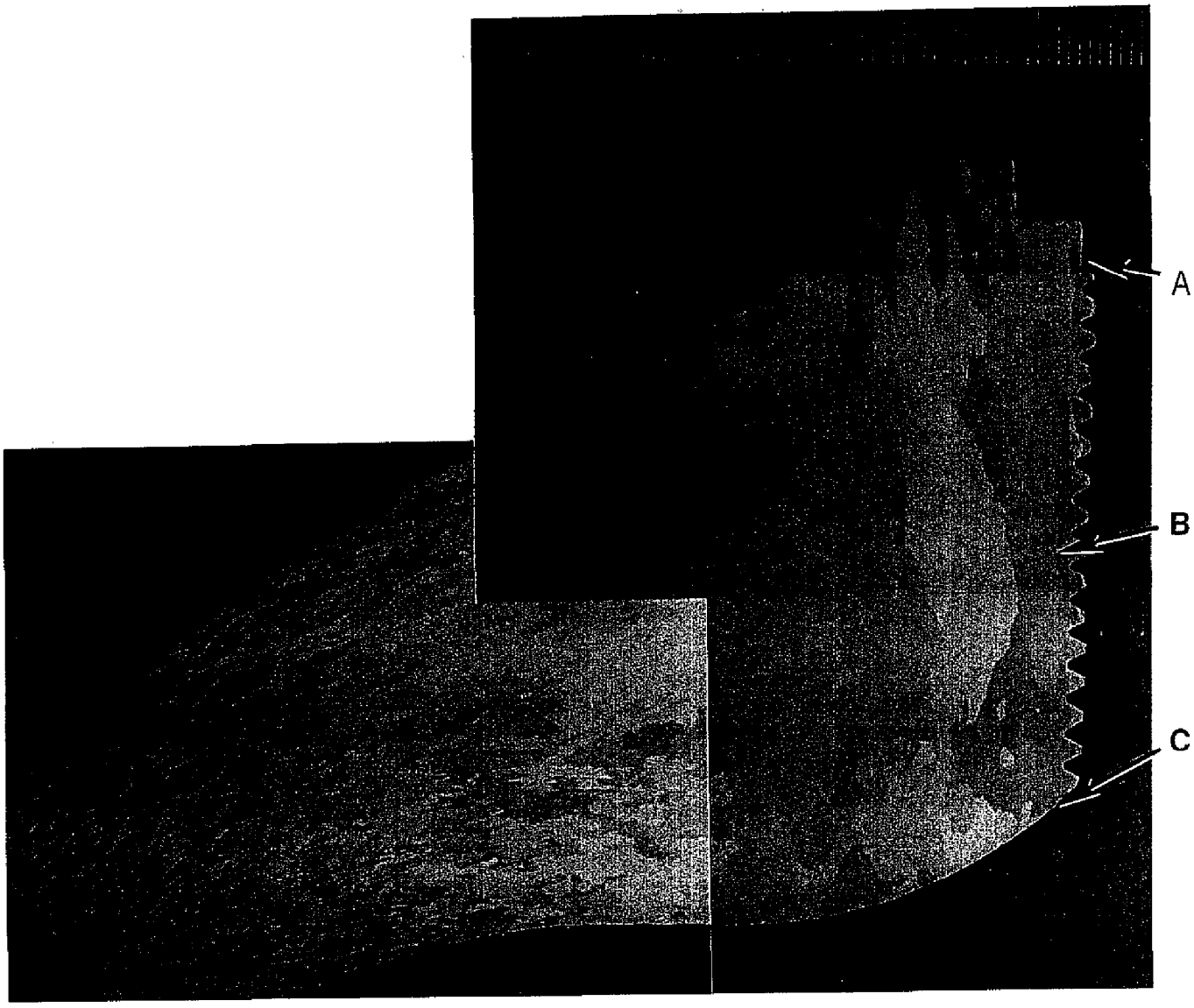

Figure 8: Section 2A-1A showing the microstructure in the neck region. Note the scale is in 0.05 inch increments. HF-H_2SO_4-H_2O etch. Photo ID: DC18128-PAL-1,2,3 8/5/98.

Regions A, B, and C are investigated further in figures 9, 10, and 11.

Figure 9: Section 2A-1A region A, photo montage. Photo ID: DC18128-Pal2, 3, 4 8/7/98.

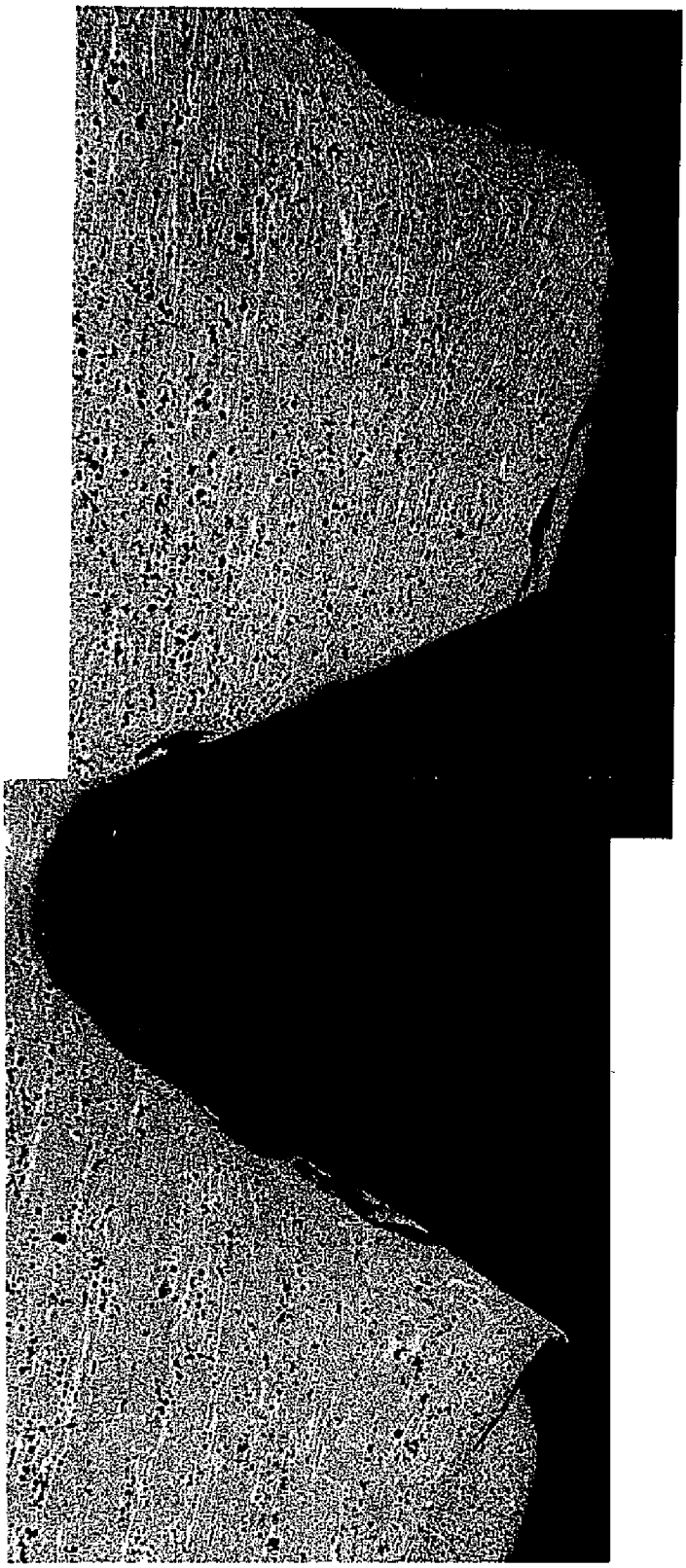

Figure 10: Section 2A-1A region B, photo montage. Photo ID: DC18128-Pal10, 11 8/7/98.

Ex.

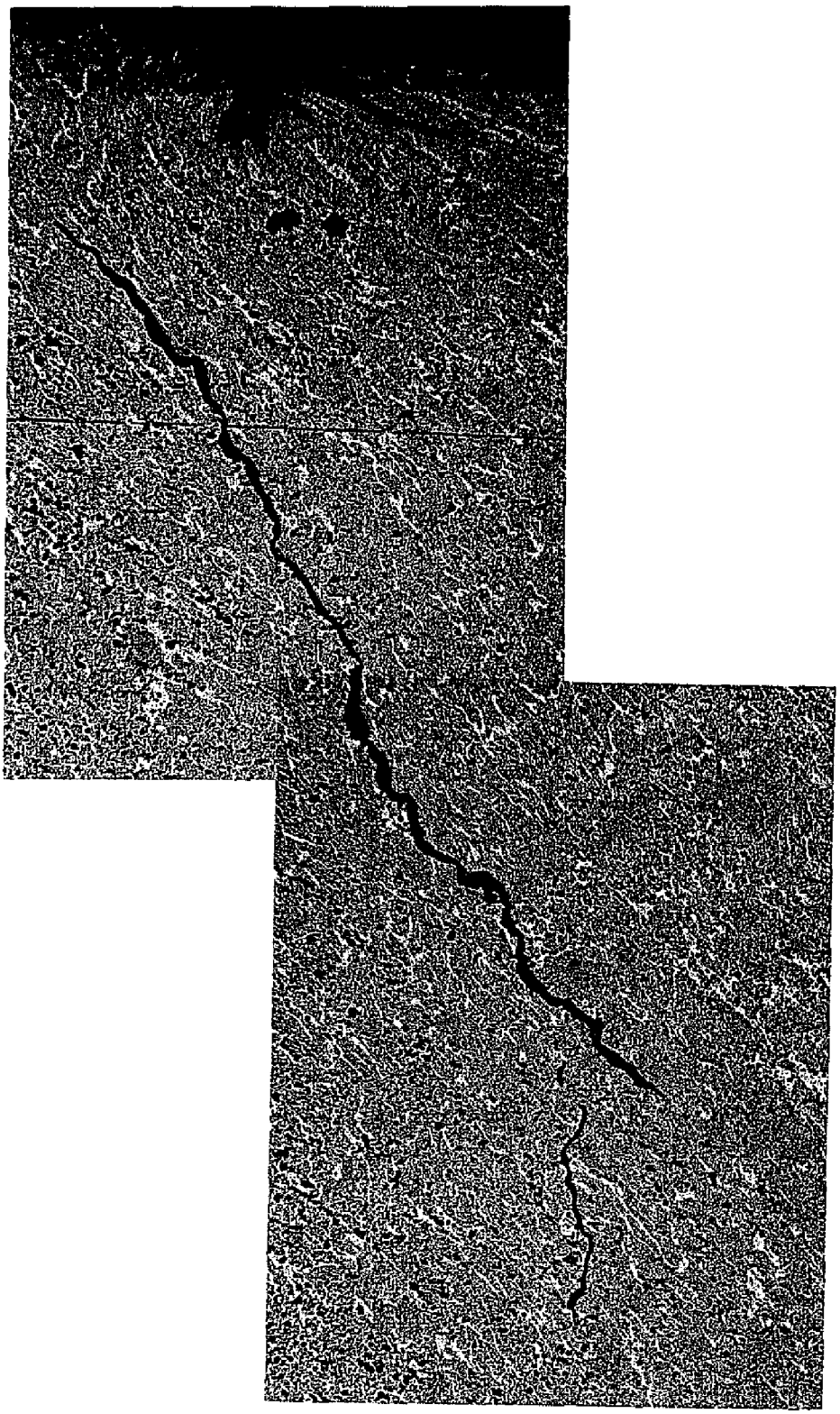

Figure 11: Section 2A-1A region C, photo montage. Photo ID: DC18128-Pal6, 7 8/7/98. Note the discontinuities in the crack.

Ex.

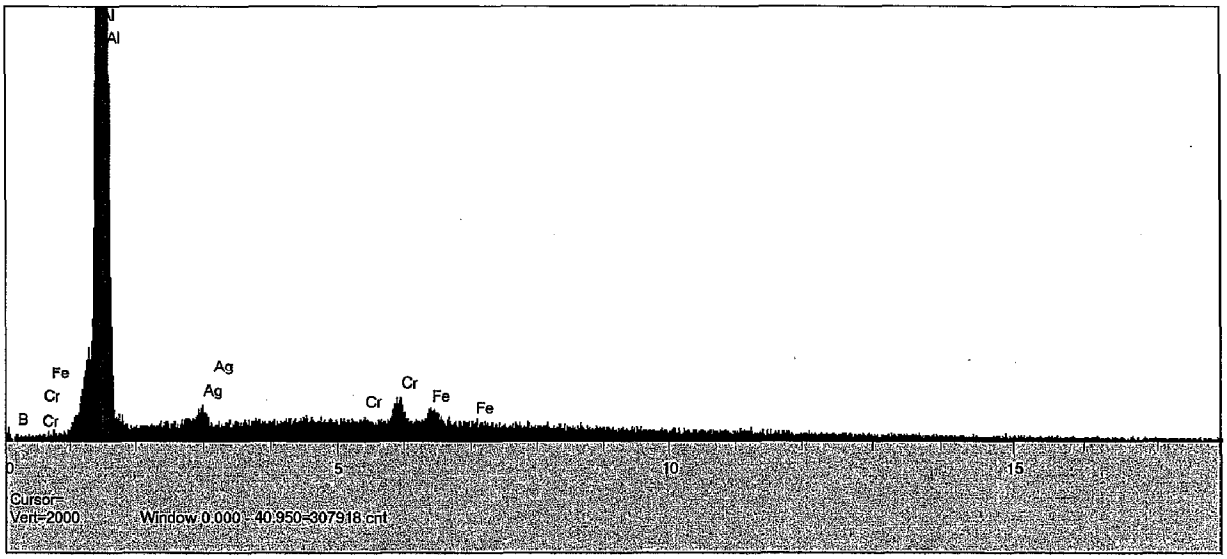

Figure 12: Energy Dispersive Spectrum taken near the corrosion product in the thread region.
Photo ID: DC18128 10/6/98 2:19:43 PM

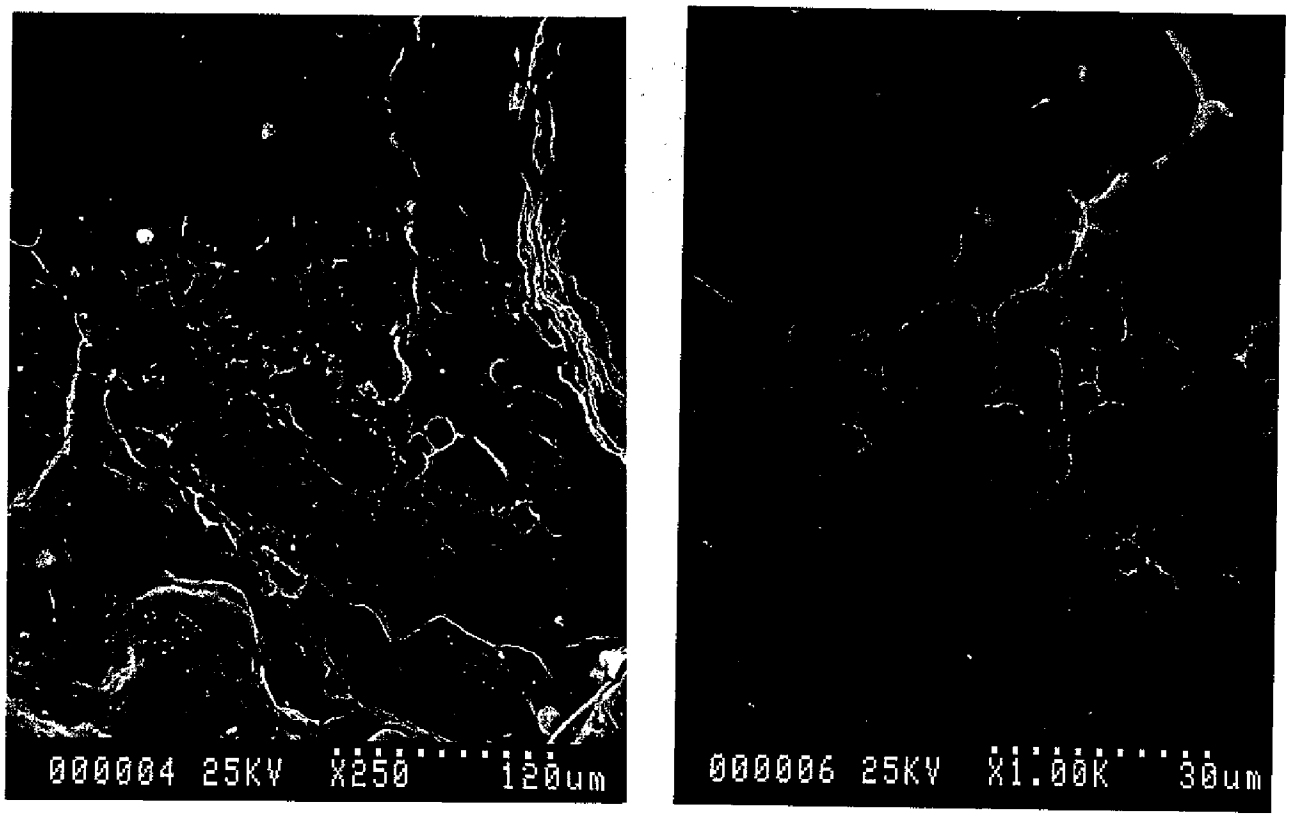

Region 1

Figure 13: Fractography of section 2A-2. Regions 1 through 5 are delineated in figure 6.

(a) Region 1. 250X. Photo ID: DC18128-PAL4 6/25/98
(b) Region 1. 1000X. Photo ID: DC18128-PAL6 6/25/98
(c) Region 2. 250X. Photo ID: DC18128-PAL8 6/25/98
(d) Region 2. 1000X. Photo ID: DC18128-PAL10 6/25/98
(e) Region 3: 250X. Photo ID: DC18128-PAL12 6/25/98
(f) Region 3: 1000X. Photo ID: Dc18128-PAL14 6/25/98
(g) Region 4. 250X. Photo ID: DC18128-PAL16 6/25/98
(h) Region 4: 500X. Photo ID: DC18128-PAL-17 6/25/98
(i) Region 4. 1000X. Photo ID: DC18128-PAL18 6/25/98
(j) Region 5. 250X. Photo ID: DC18128-PAL20 6/25/98
(k) Region 6. 1000X. Photo ID: DC18128-PAL21 6/25/98

Ex.

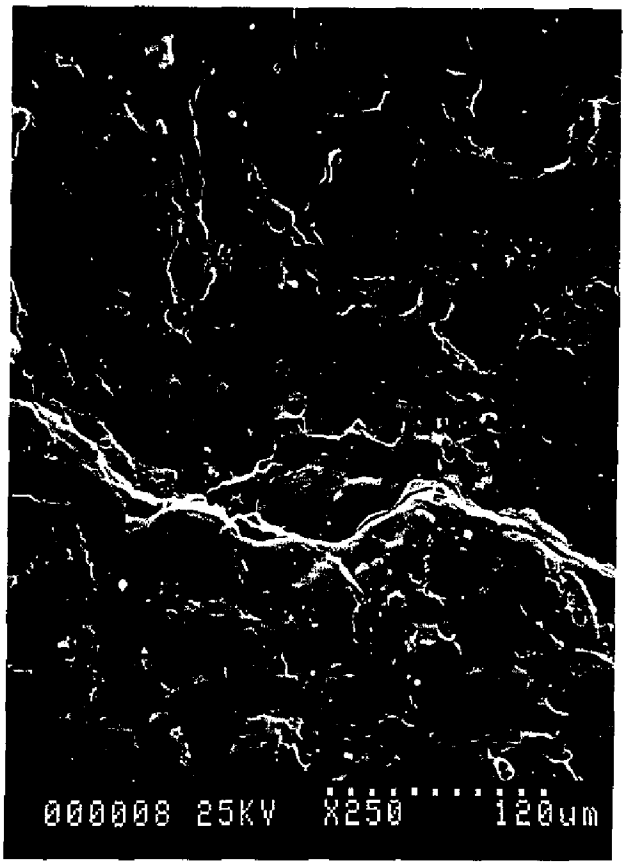

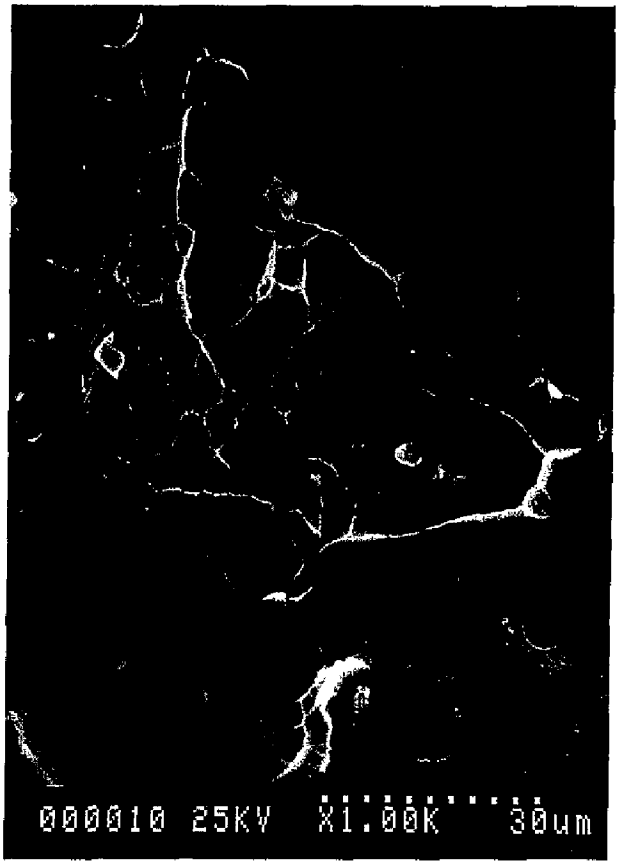

Region 2

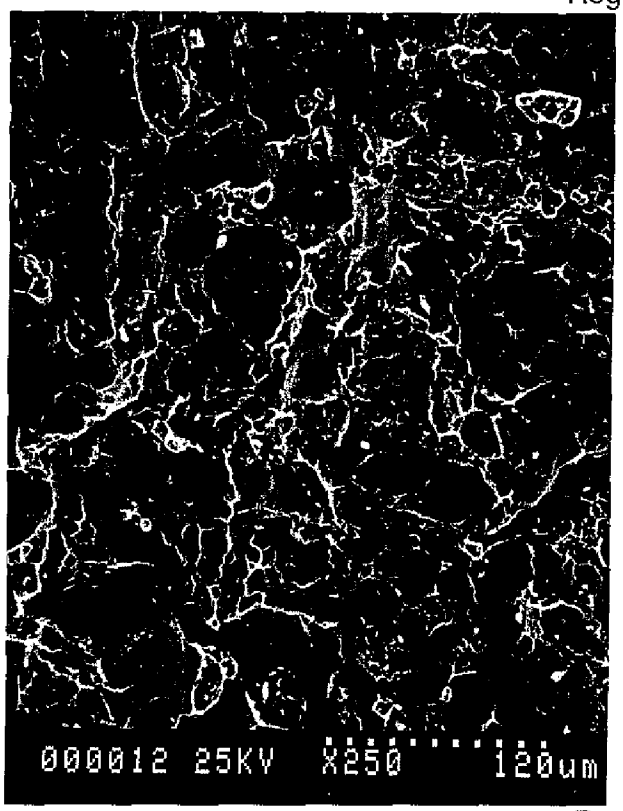

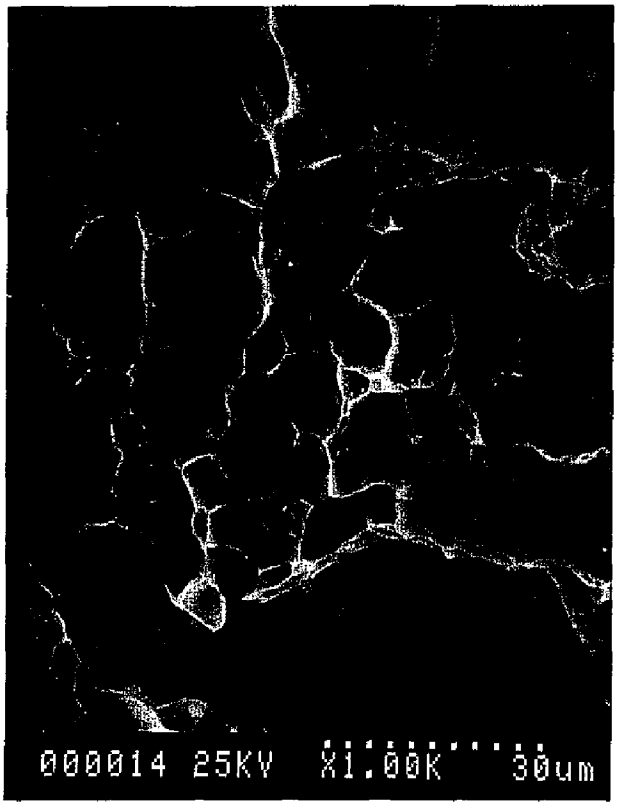

Region 3

Ex.

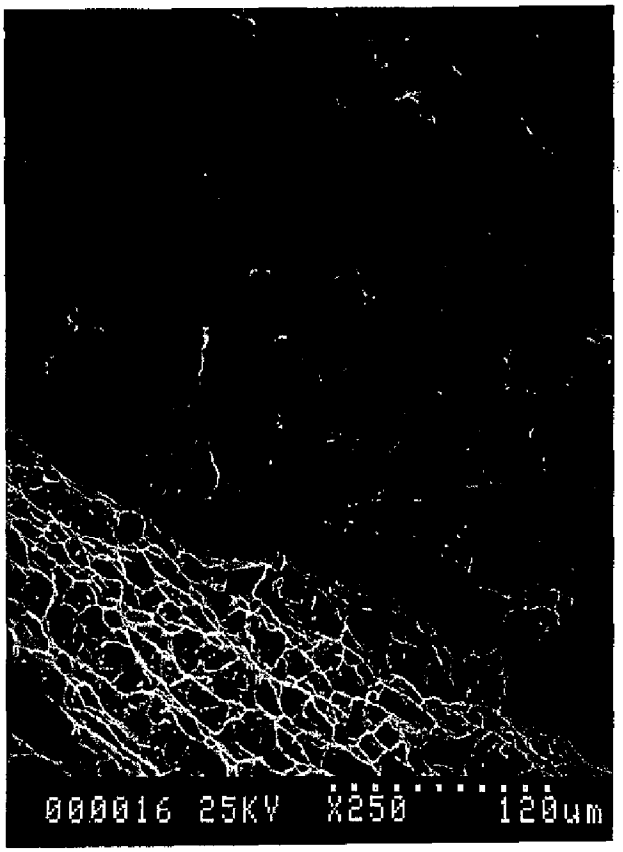
000016 25KV X250 120um

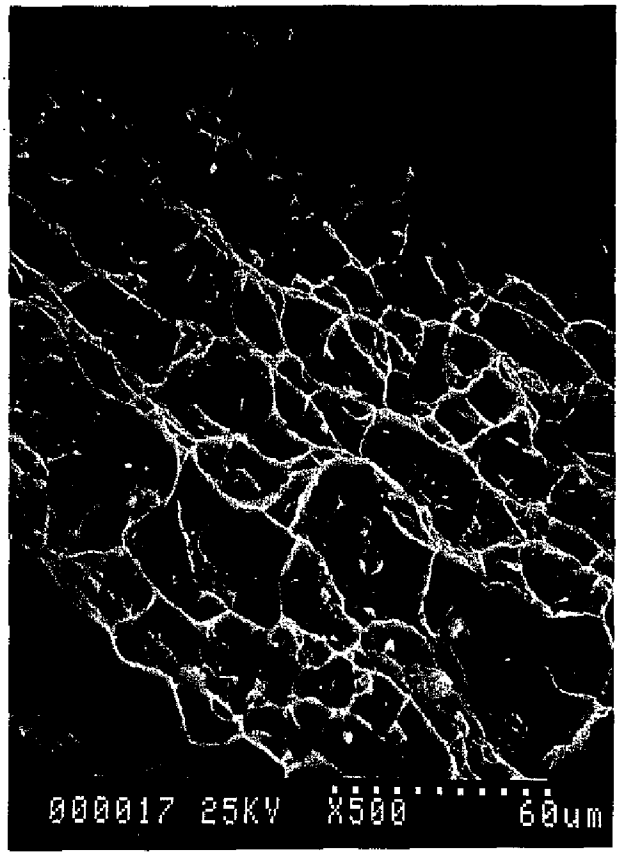
000017 25KV X500 60um

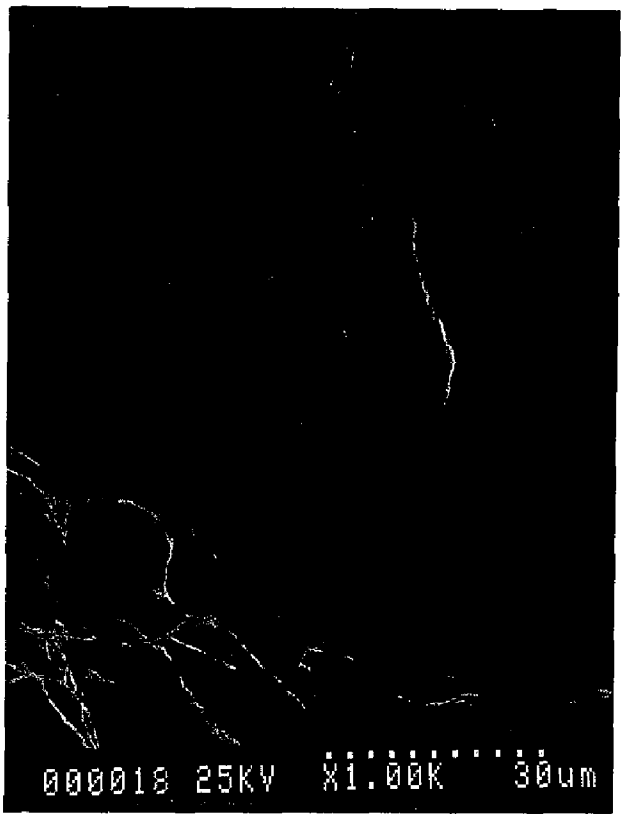
000018 25KV X1.00K 30um

Region 4

Ex.

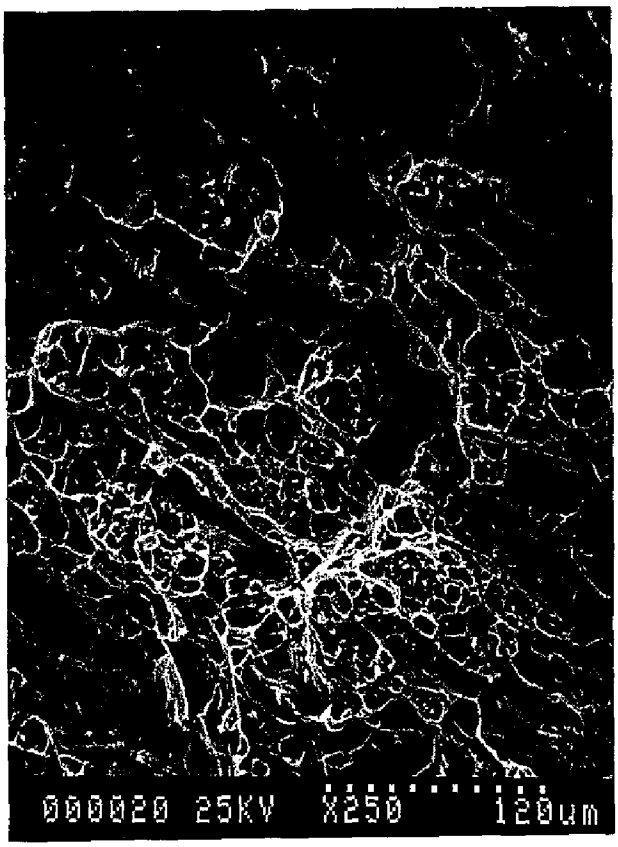

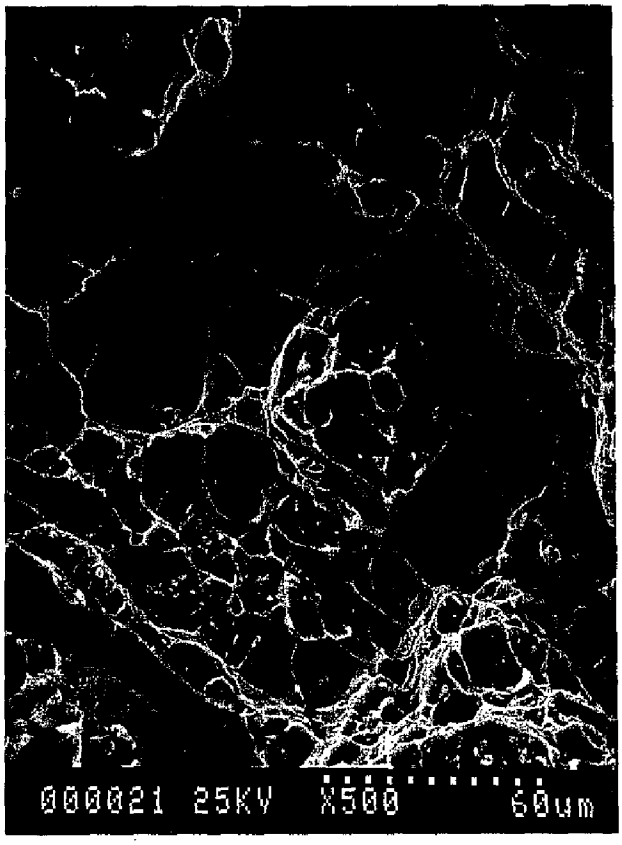

Region 5

Ex.

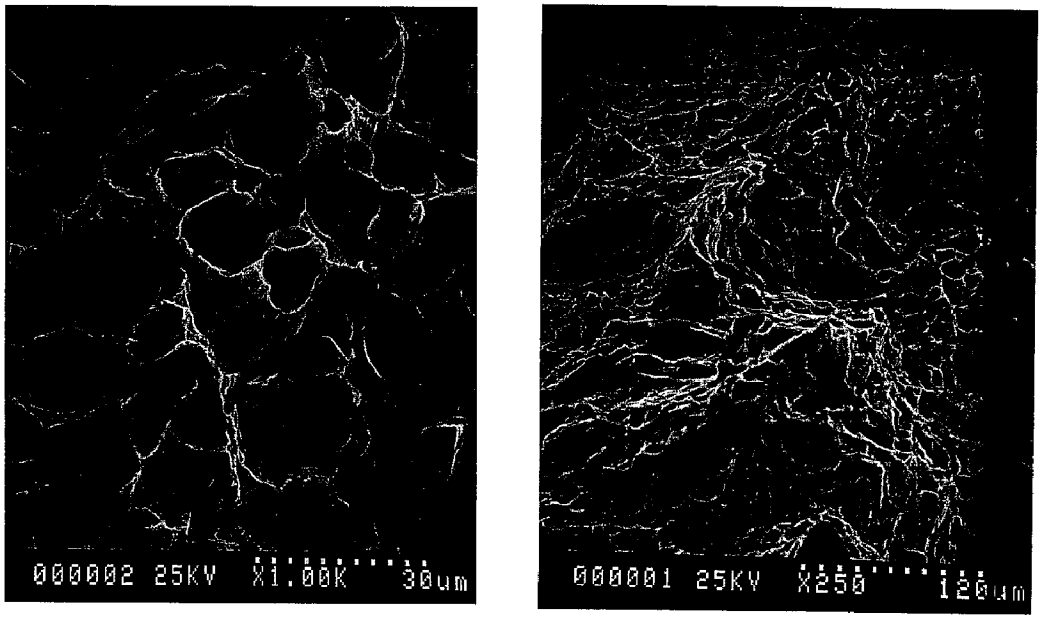

Figure 14: SEM fractographs of a tensile specimen.
(a) 250X. Photo ID: DC18128-PAL2 9/30/98
(b) 1000X. Photo ID: DC18128-PAL3 9/30/98

Appendix A: Workscope

Recommended Scope of Work for Metallurgical Evaluation of Aluminum Cylinder

1. Photodocumentation. Prior to any destructive examination of this cylinder, it will be photodocumented to illustrate its "as-received" condition. After each cutting operation needed to remove samples for testing or evaluation (such as required for chemical samples) the cylinder and sample will be photodocumented to illustrate the sample location. Photodocument the primary fracture surface as well as any secondary cracks that may be present. Any corrosion deposits or other visible surface contaminants should also be photodocumented.
2. Corrosion. Testing for corrosion product should be done prior to any extensive cutting or handling of the cylinder remains. Swipe samples or cutting of material containing any such potential corrosion products should be taken. When cutting is performed, care should be used to minimize contamination of the cylinder surfaces. Swipe samples or samples containing potential corrosion products should first be analyzed by scanning electron microscopy and energy dispersive spectroscopy (SEM/EDS).
3. Chemical Analysis. The cylinder aluminum alloy will be analyzed for chemical composition to compare with materials specifications. Material from the neck region, side wall, and cylinder bottom will be analyzed to check for alloy homogeneity. The analysis will also determine the concentration of potentially detrimental trace elements, such as lead.
4. Macroetching. A thin slice of material will be removed from the neck of the cylinder that includes sidewall material. This slice will be macroetched to show the grain macro/microstructure in this area.
5. Fractography. SEM and stereo-microscopic examination should be performed on all fractures. Particular attention should be focused in the regions where the fracture originated. Any indication of fatigue, stress-corrosion cracking, ductile rupture, inter/intra-granular fracture features, etc., should be photodocumented.
6. Dimensional Checking. Prior to extensive cutting, the cylinder wall thickness at various locations and other cylinder features, such as threads, cylinder internal diameter, inlet hole diameter should be measured. Measurements done should be sufficient to determine the minimum wall thickness as well as to document any extensive plastic tearing that may have resulted in the failure event.
7. Secondary Cracking. A section of the primary fracture surface near the crack origin should b metallographically polished. Any secondary cracking near the failure origin should be evaluated. These sections should be first examined in the unetched condition and photodocumented to look for crack branching. The sample should then be etched, re-examined, and photodocumented.
8. Material Hardness. The material hardness shall be evaluated in the neck, wall, and cylinder bottom by means of macrohardness testing according to ASTM standards.
9. Physical Testing. Mechanical test per 49 CFR 178.46-5
10. Report. Report should contain a description of all tests performed and the results obtained. If possible, state the location of the crack origin, mode of fracture, and likely cause of failure.

Appendix B: Complete Photodocumentation

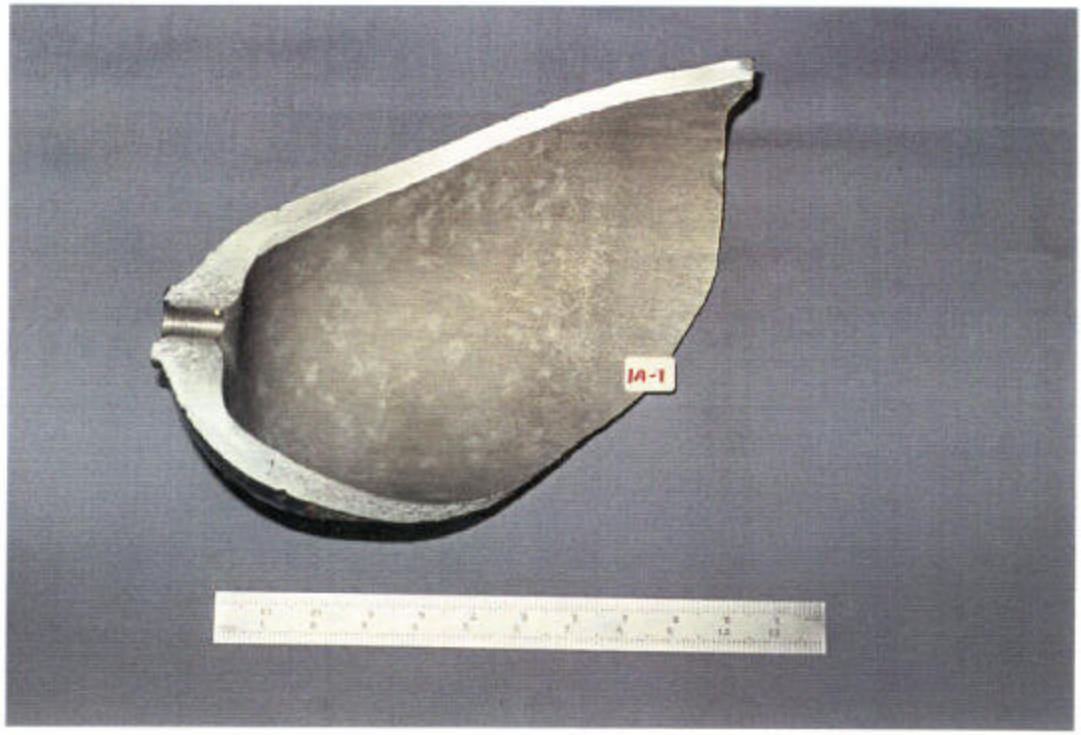

Photo ID: DC18128-R1E2

Photo ID: DC18128-R1E3

Ex.

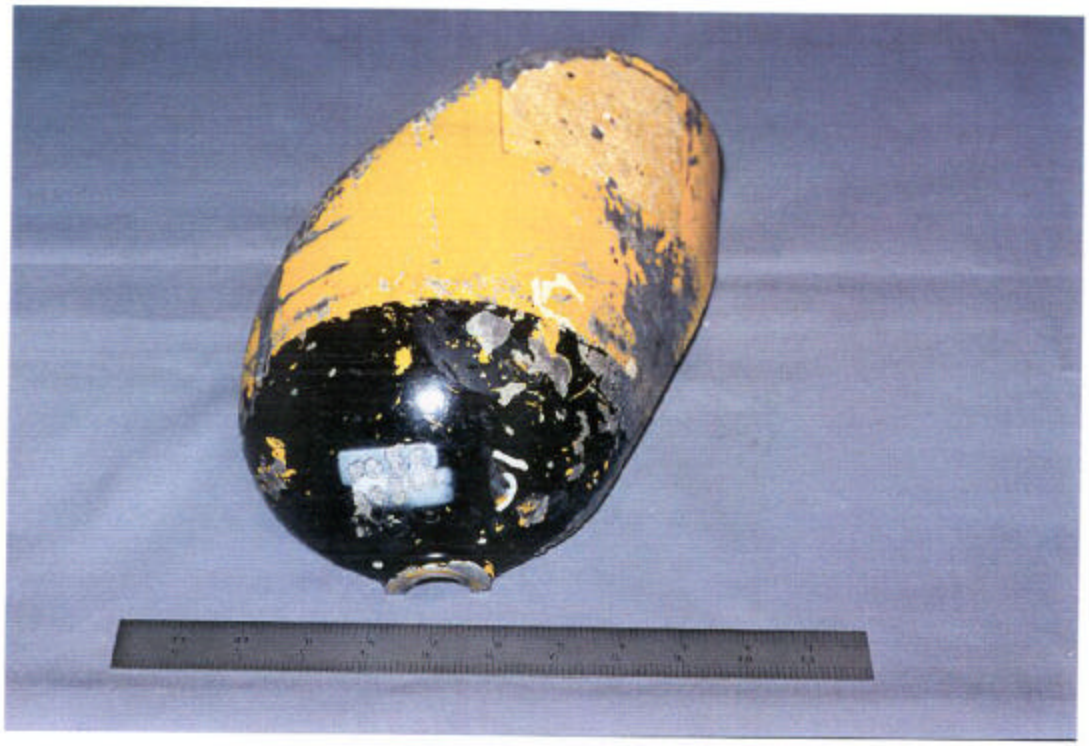

Photo ID: DC18128-R1E4

Photo ID: DC18128-R1E5

Ex.

Photo ID: DC18128-R1E6

Photo ID: DC18128-R1E7

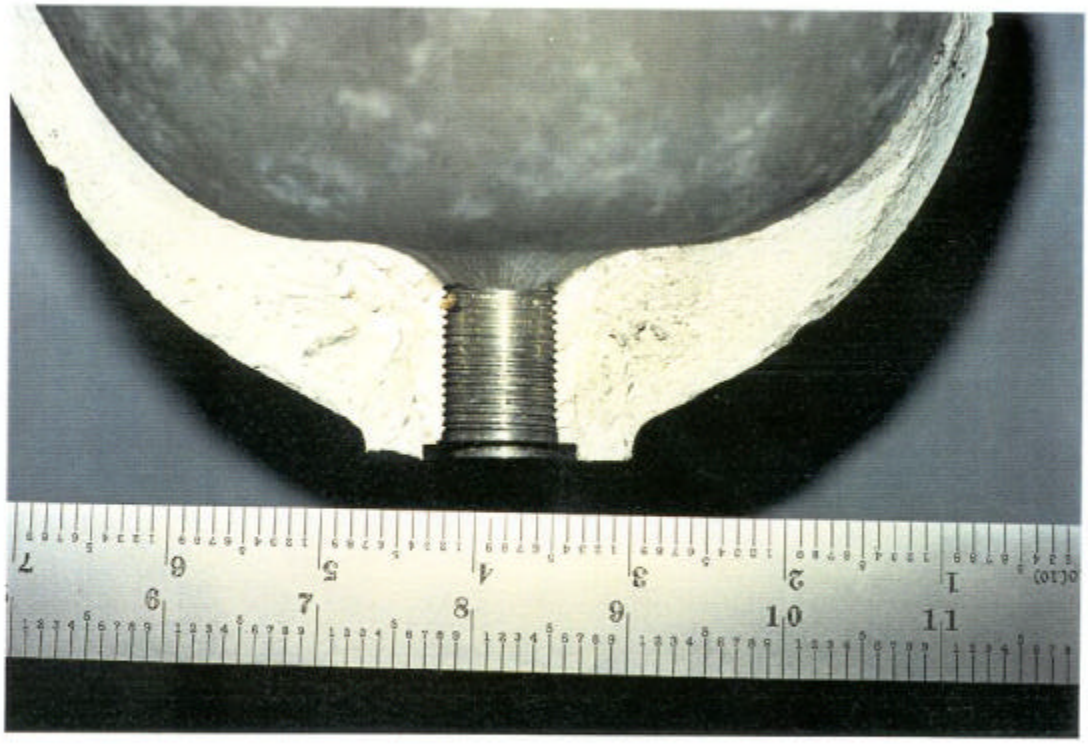

Photo ID: DC18128-R1E8

Photo ID: DC18128-R1E9

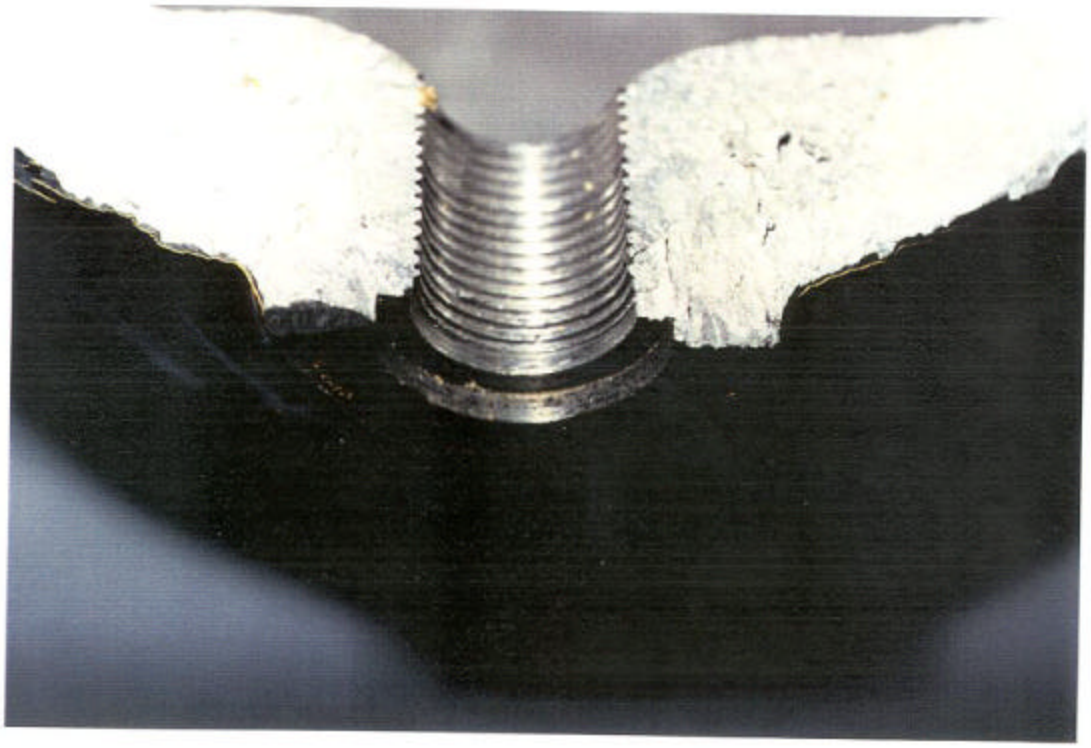

Photo ID: DC18128-R1E10

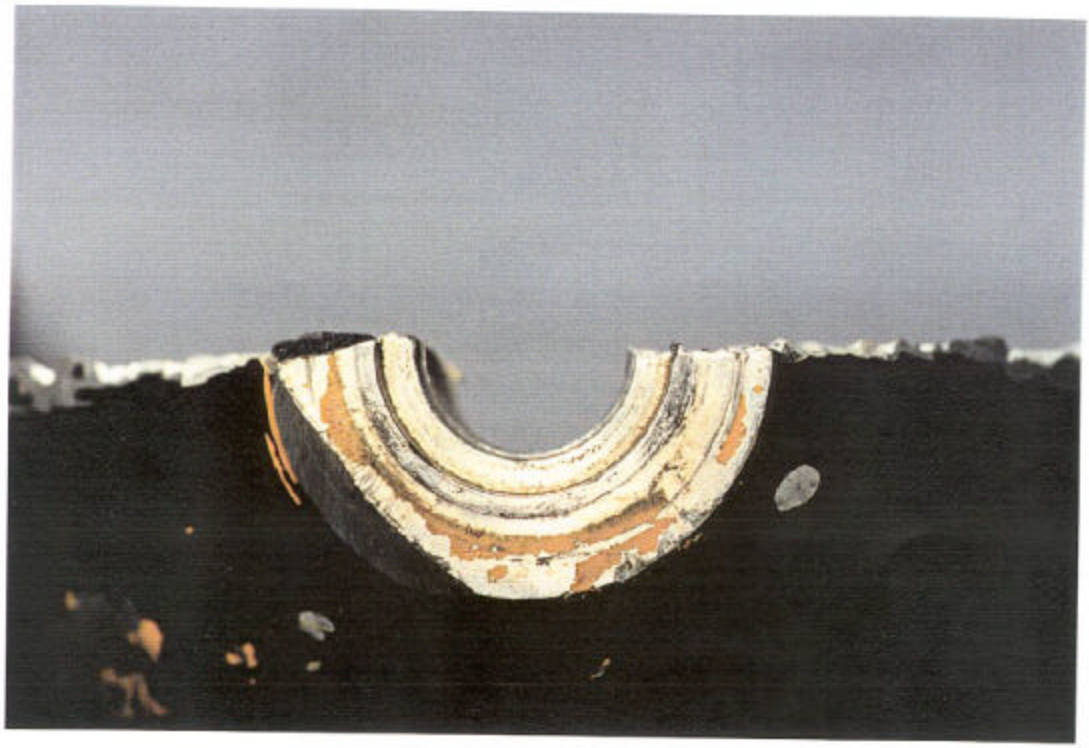

Photo ID: DC18128-R1E11

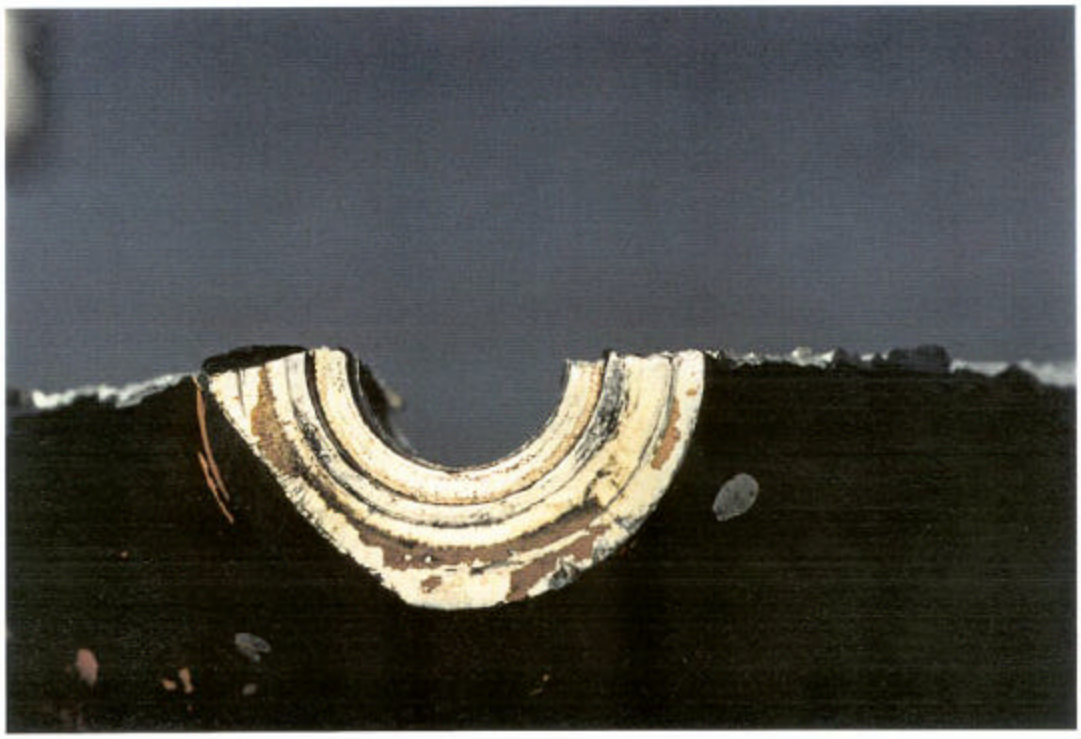

Photo ID: DC18128-R1E12

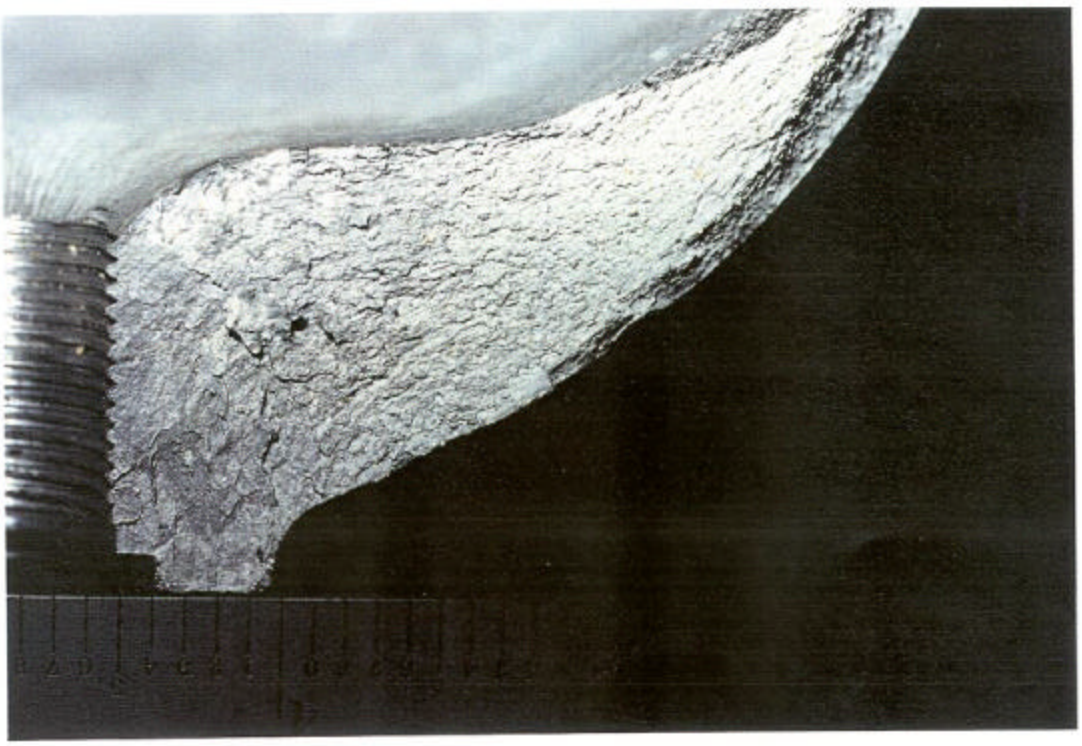

Photo ID: DC18128-R1E13

Photo ID: DC18128-R1E14

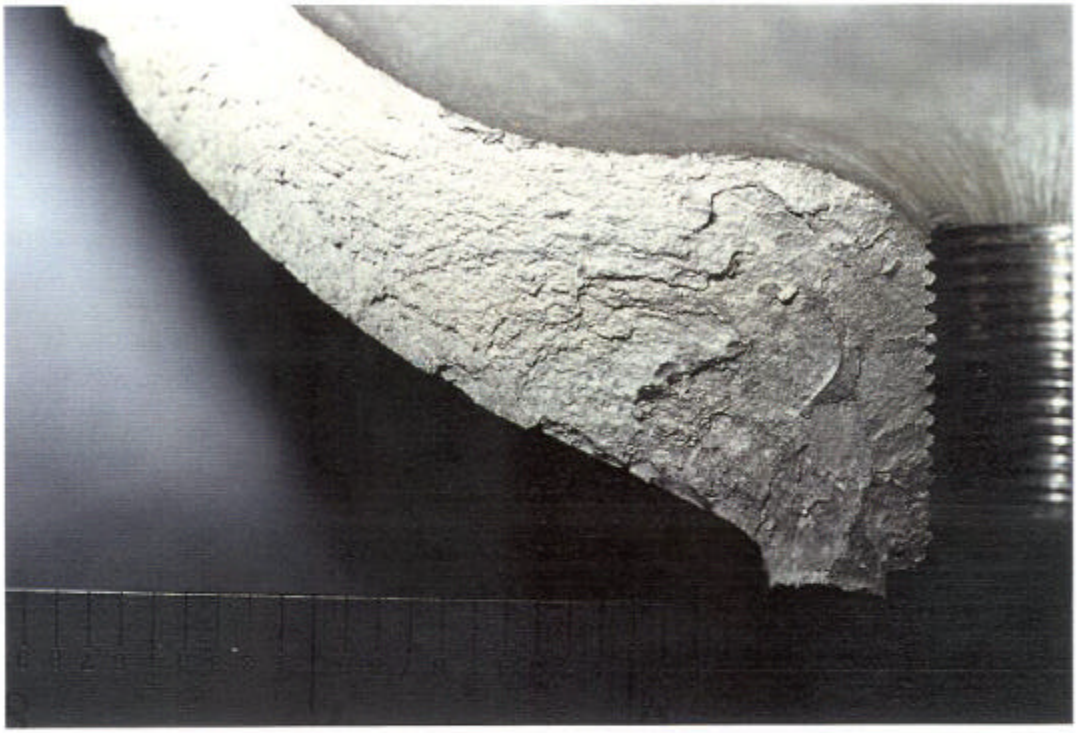

Photo ID: DC18128-R1E15

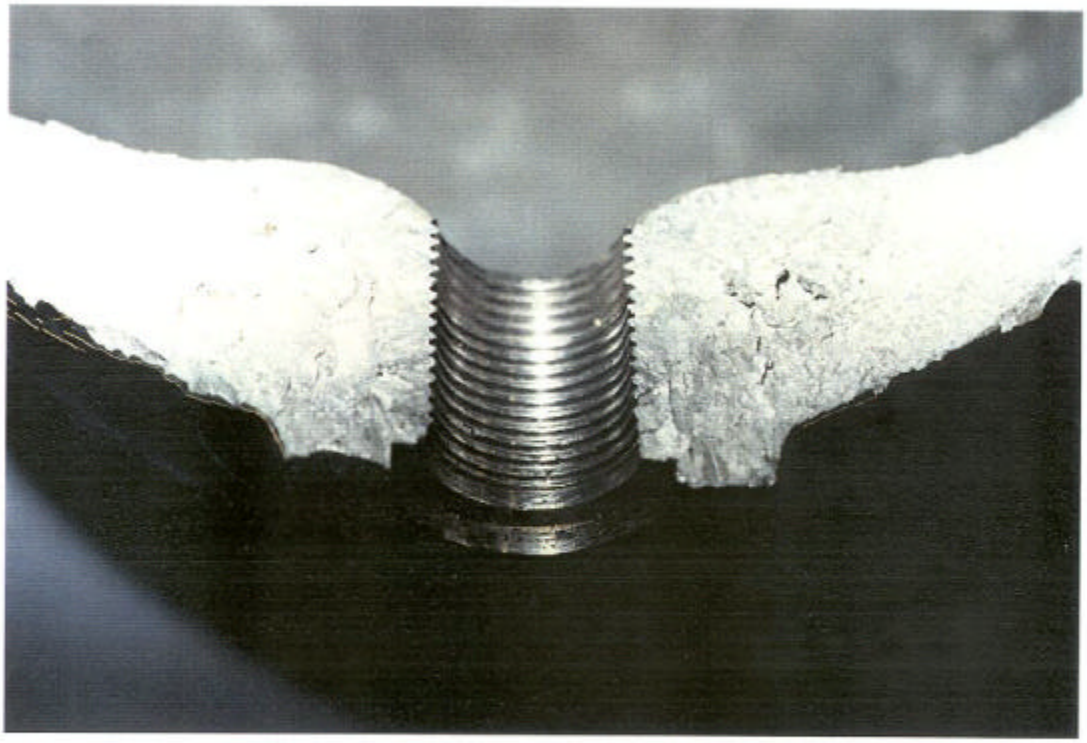

Photo ID: DC18128-R1E16

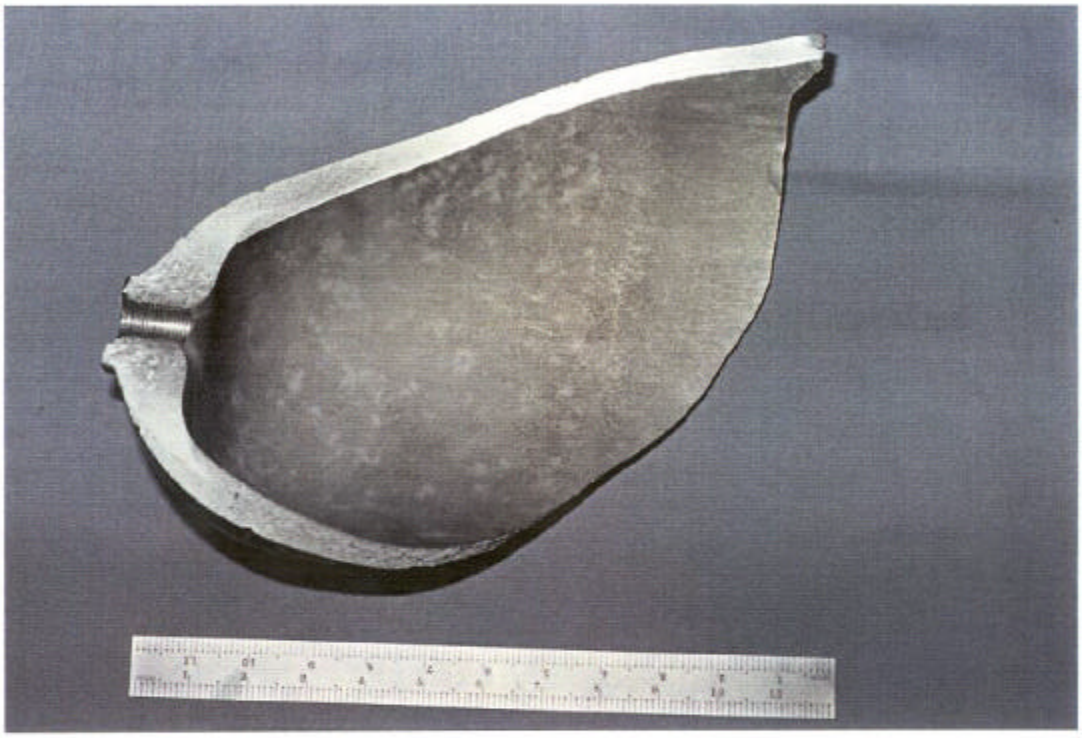

Photo ID: DC18128-R1E17

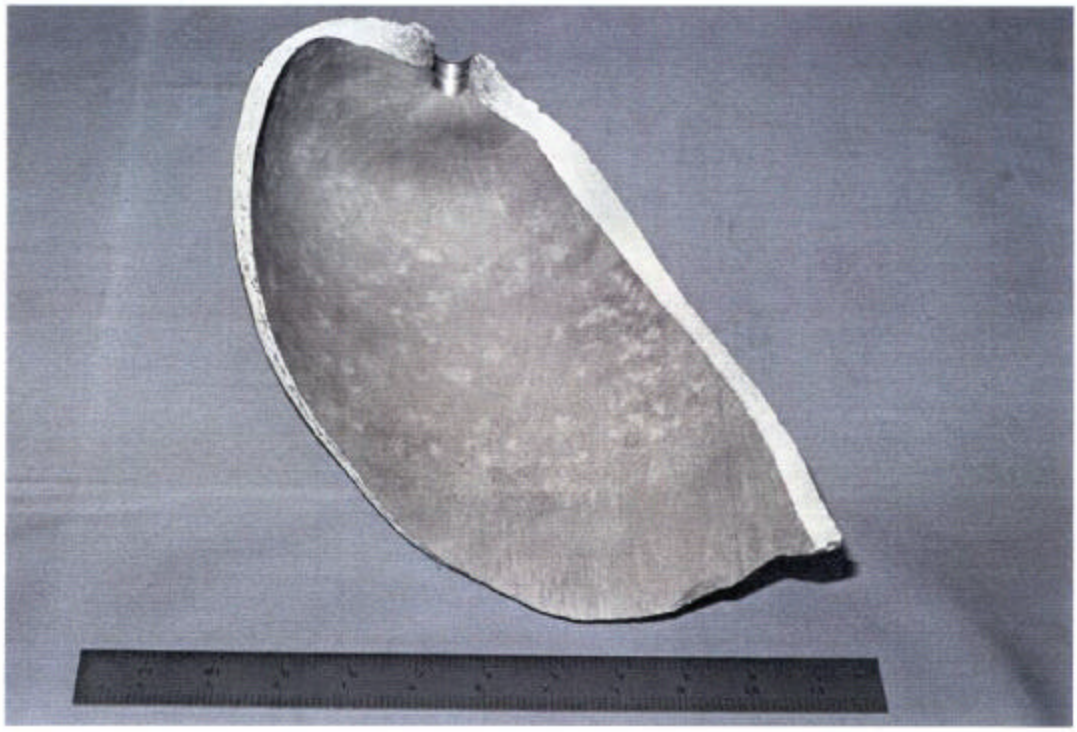

Photo ID: DC18128-R1E18

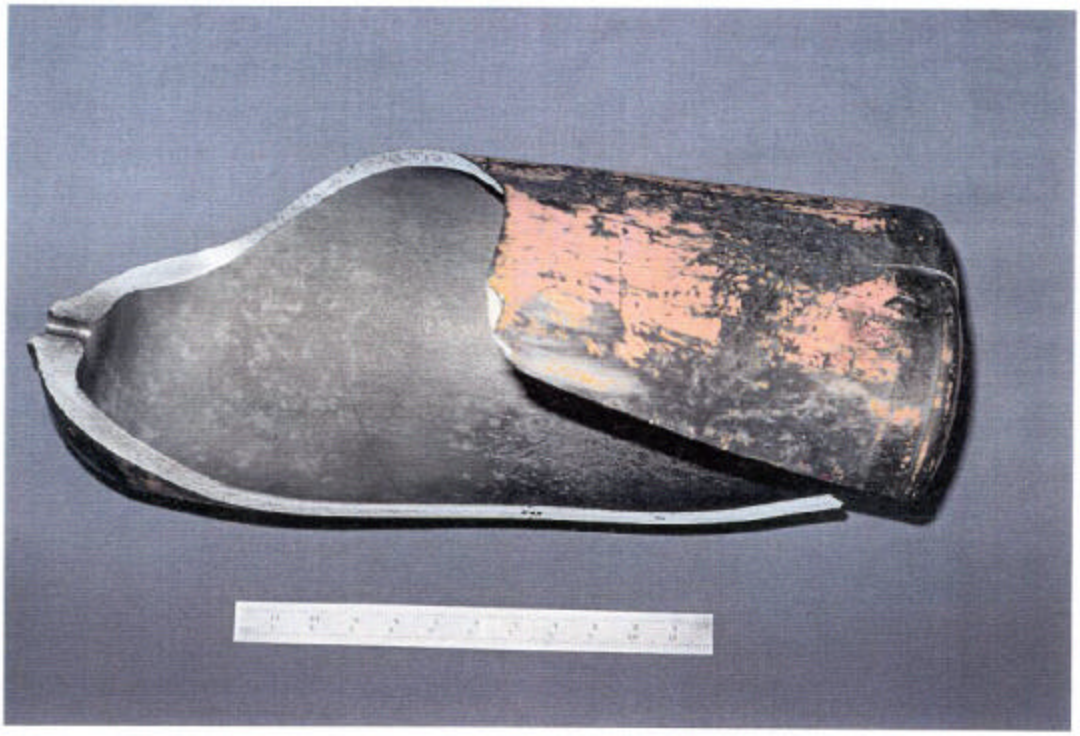

Photo ID: DC18128-R1E19

Photo ID: DC18128-R1E20

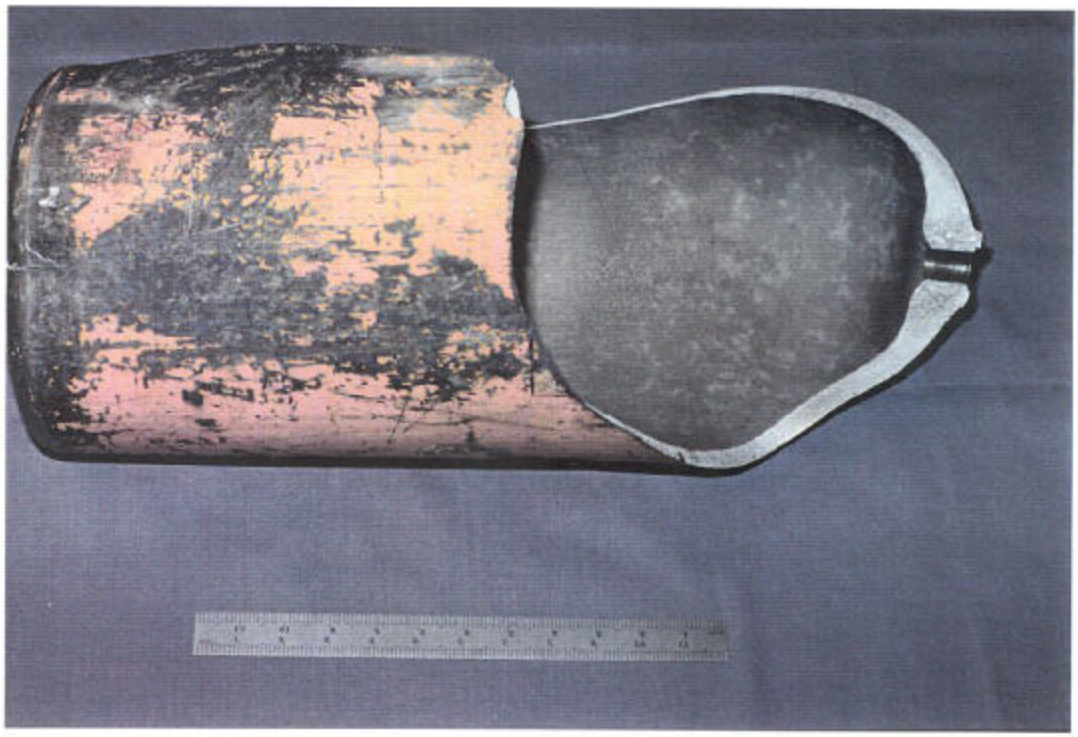

Photo ID: DC18128-R1E21

Ex.

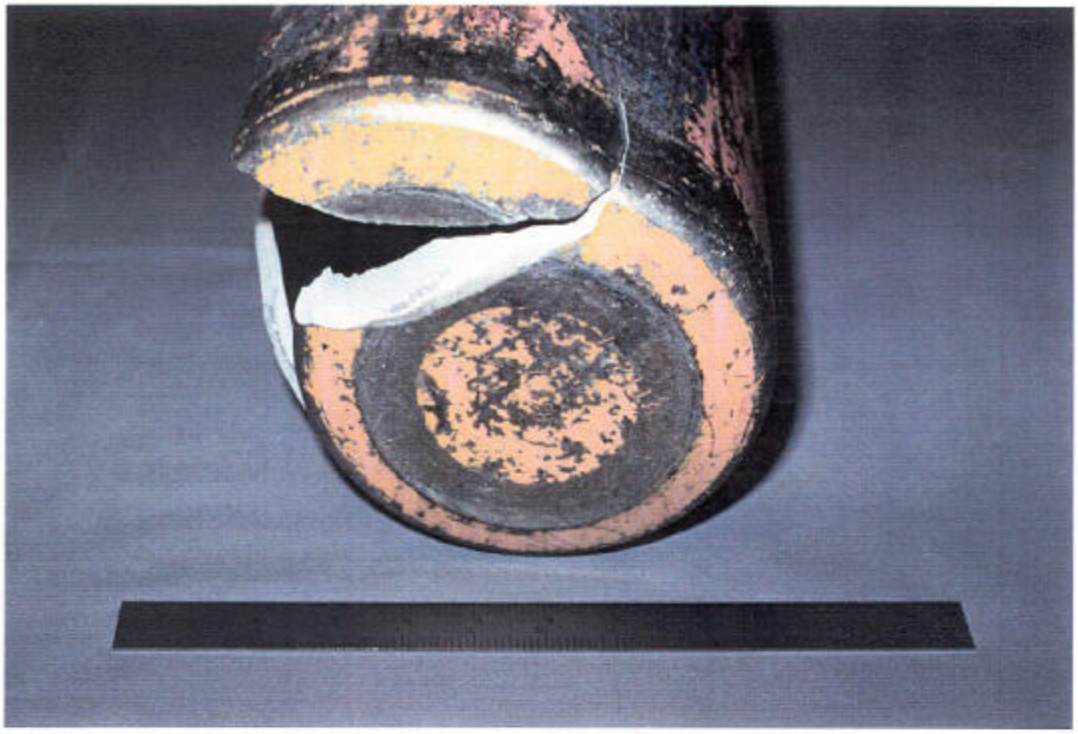

Photo ID: DC18128-R1E22

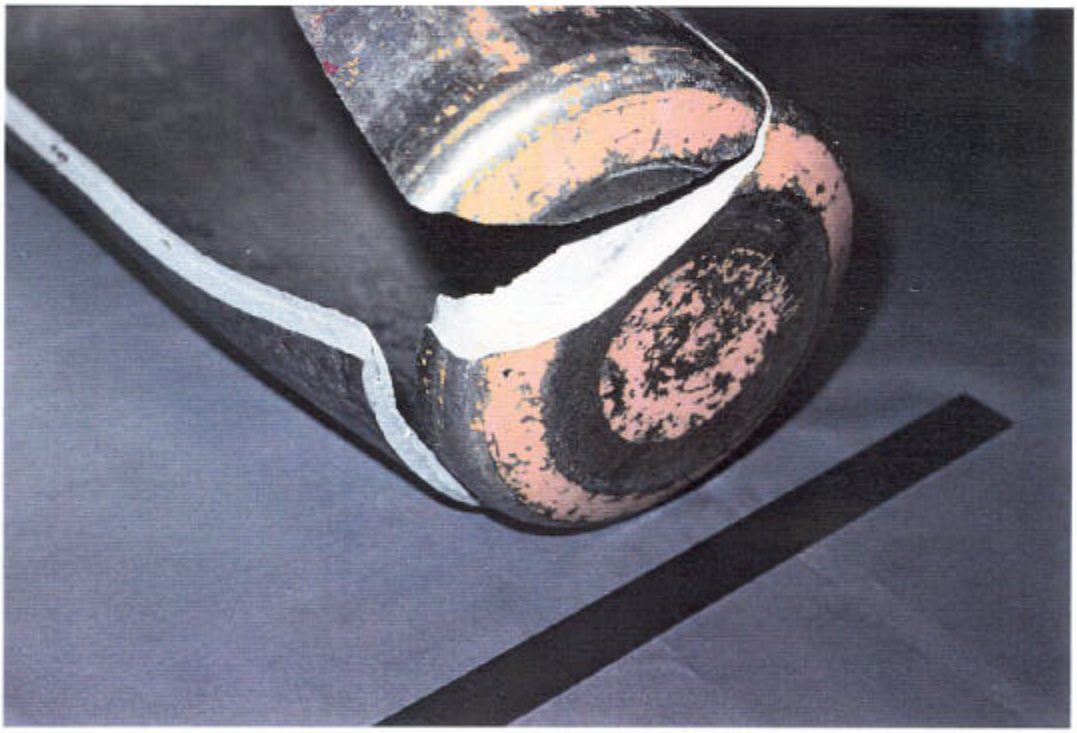

Photo ID: DC18128-R2E23

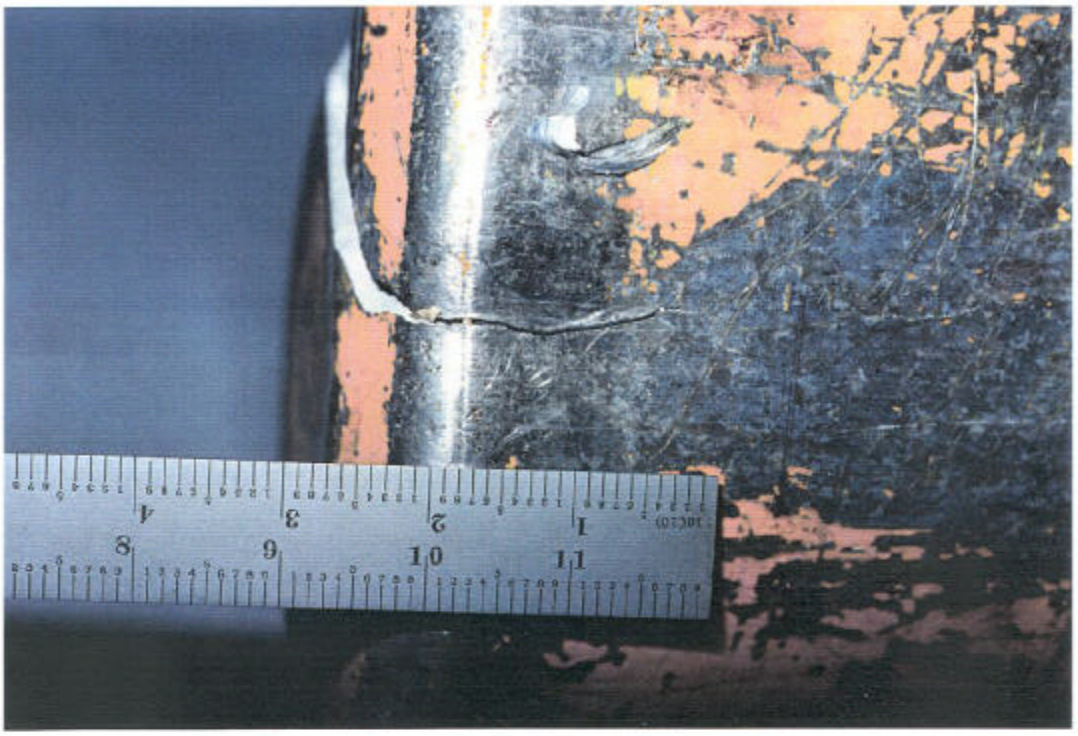

Photo ID: DC18128-R1E24

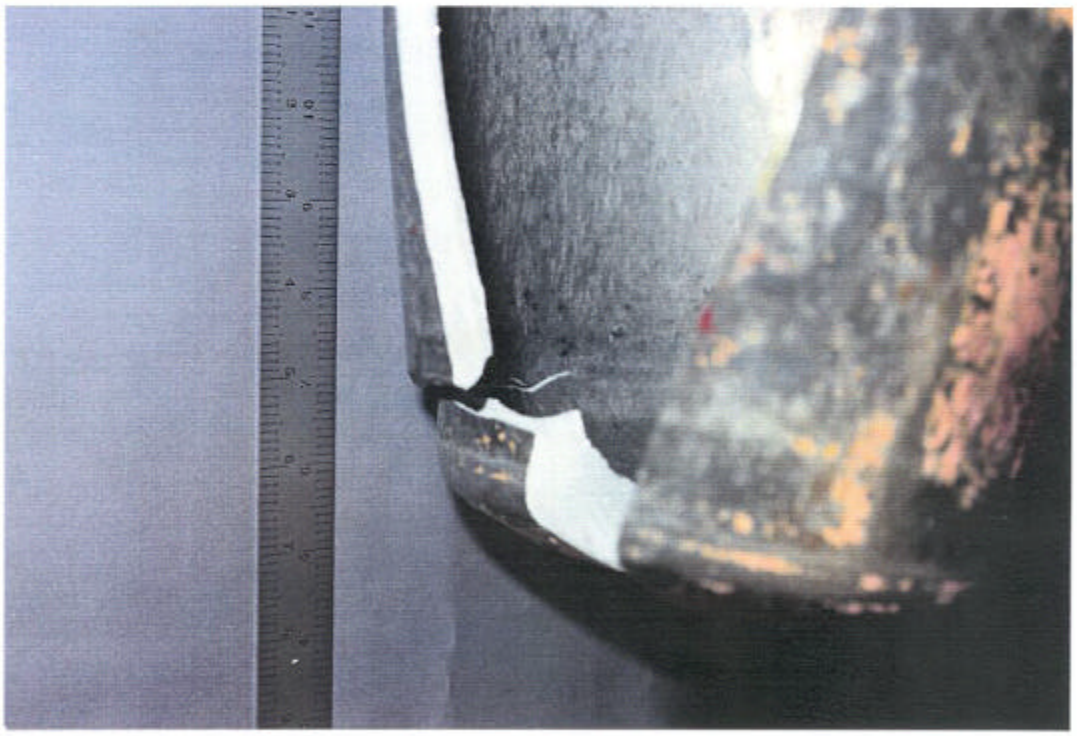

Photo ID: DC18128-R2E3

Photo ID: DC18128-R2E4

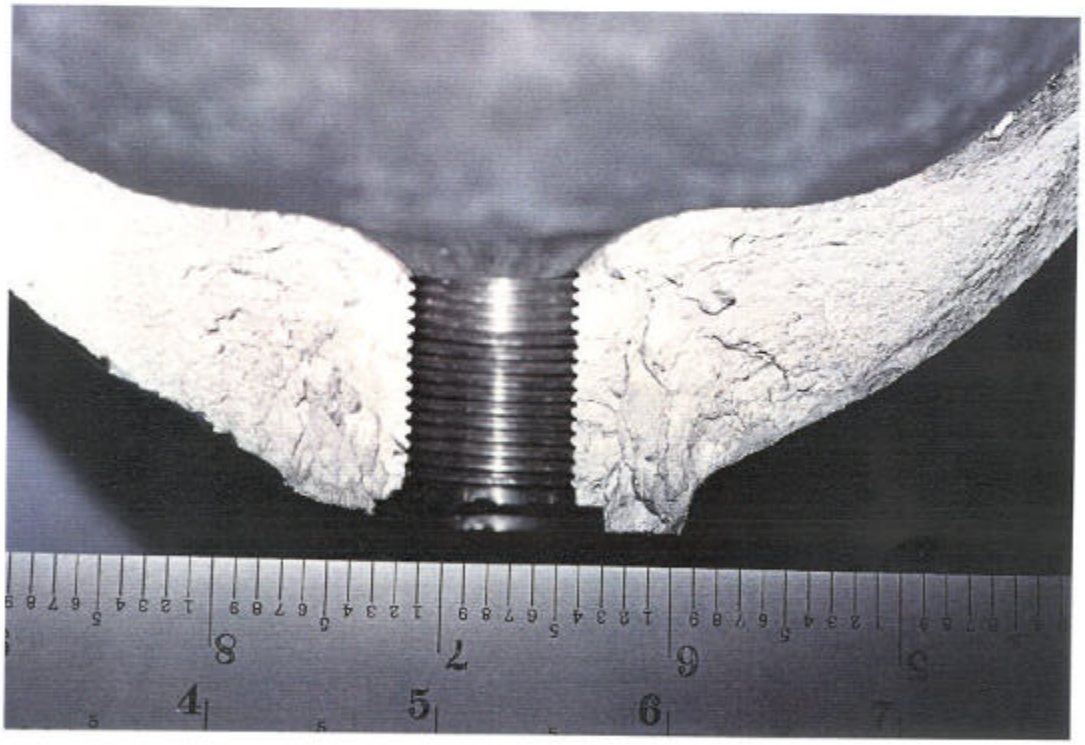

Photo ID: DC18128-R2E5

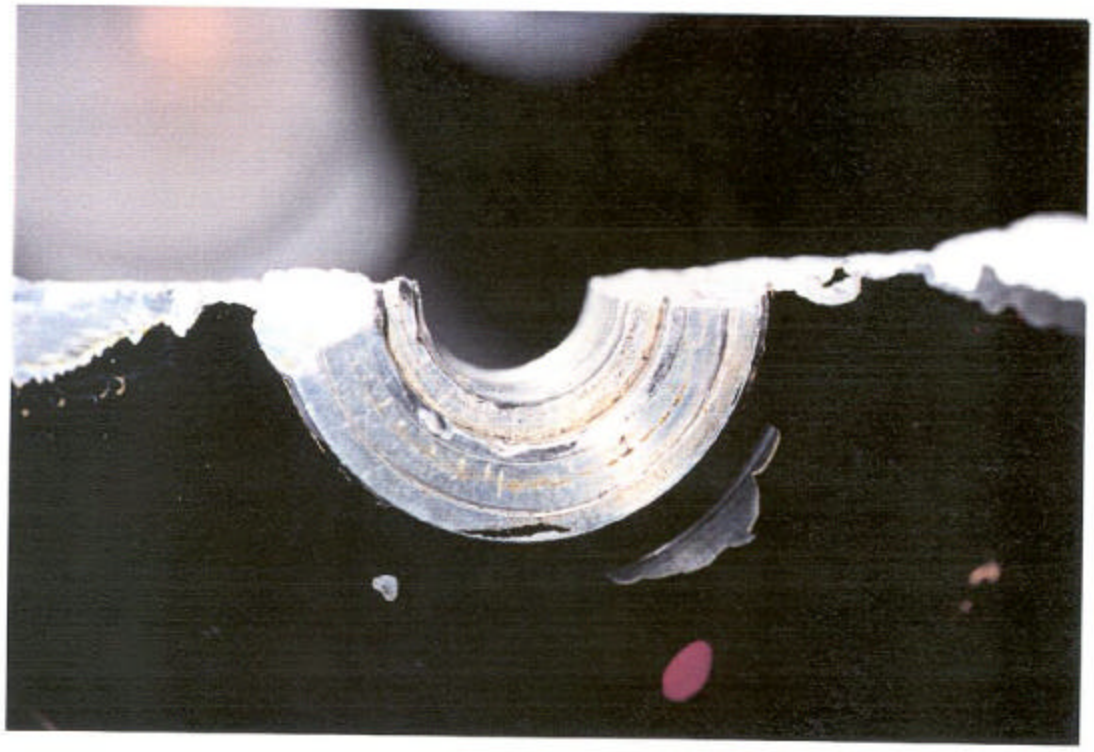

Photo ID: DC18128-R2E6

Photo ID: DC18128-R2E7

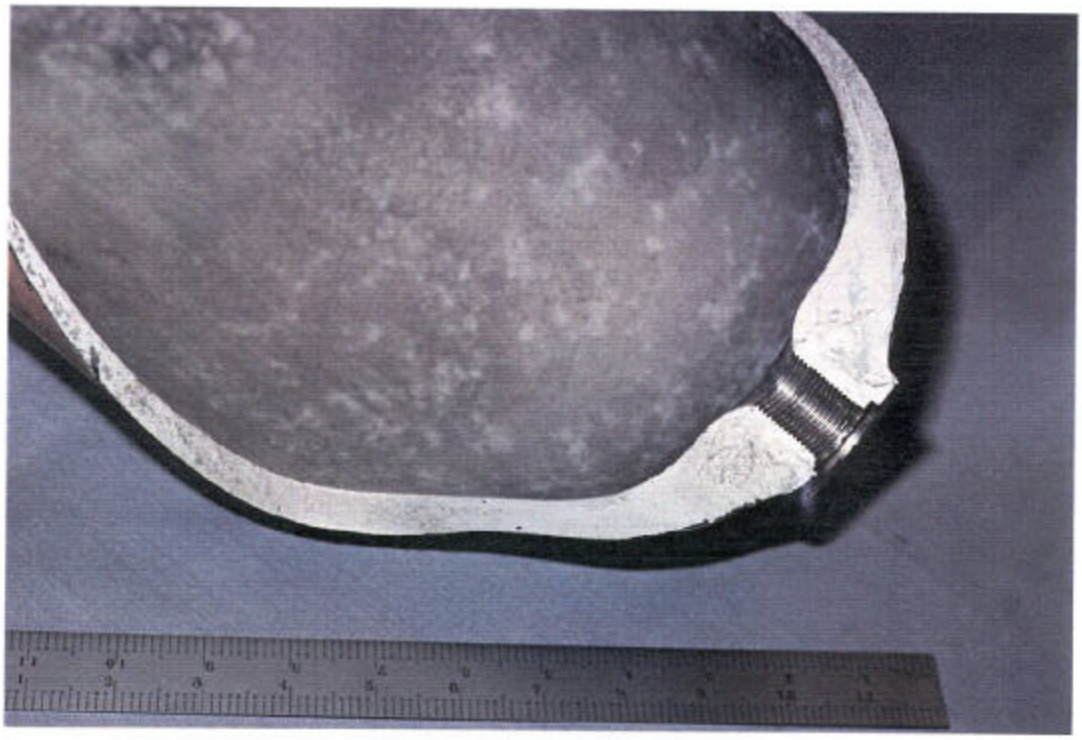

Photo ID: DC18128-R2E8

Photo ID: DC18128-R2E9

Photo ID: DC18128-R2E10

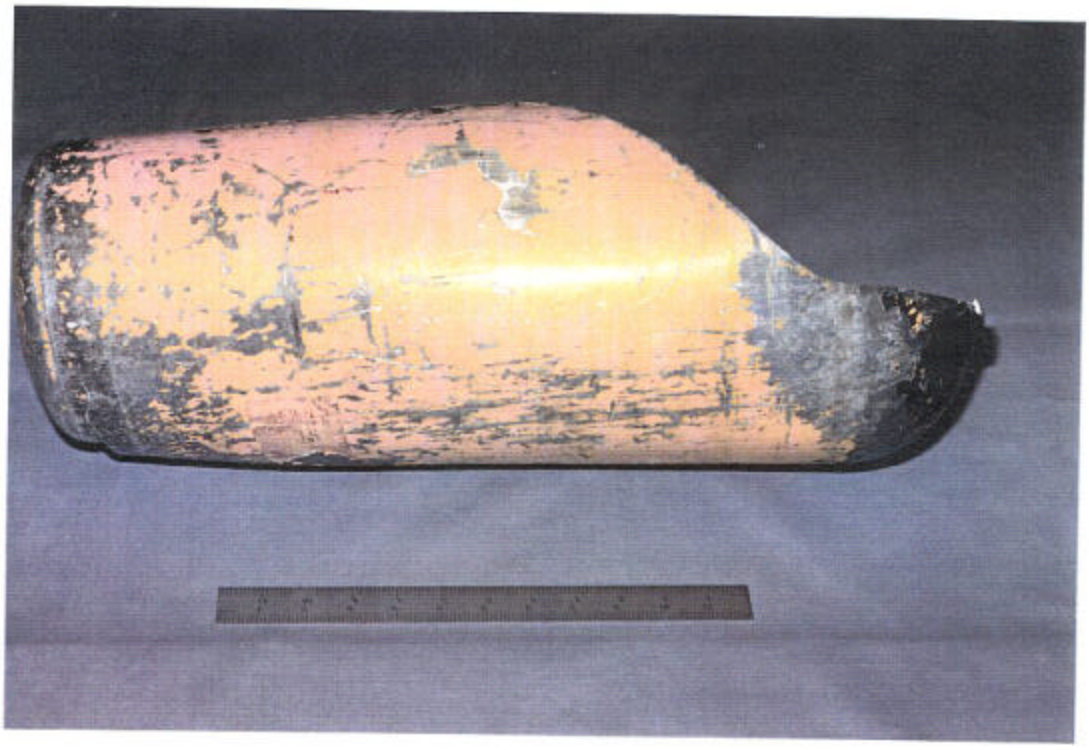

Photo ID: DC18128-R2E11

Ex.

Photo ID: DC18128-R2E12

Photo ID: DC18128-R2E13

Photo ID: DC18128-R2E14

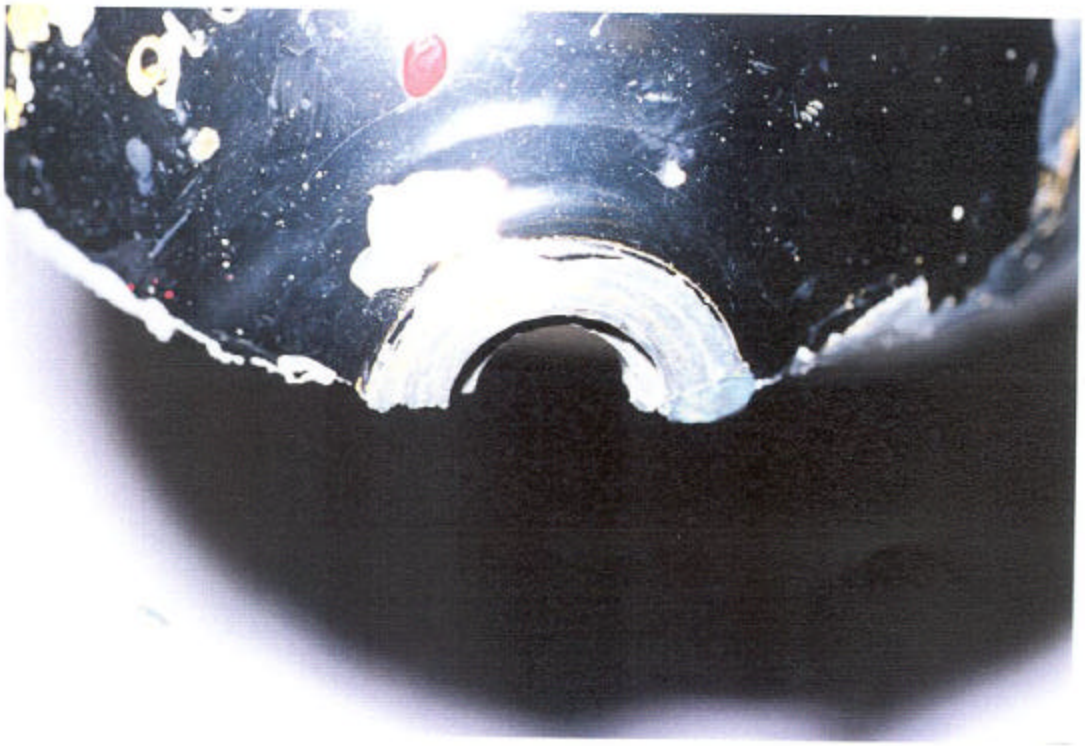

Photo ID: DC18128-R2E15

Photo ID: DC18128-R2E16

Photo ID: DC18128-R2E17

Ex.

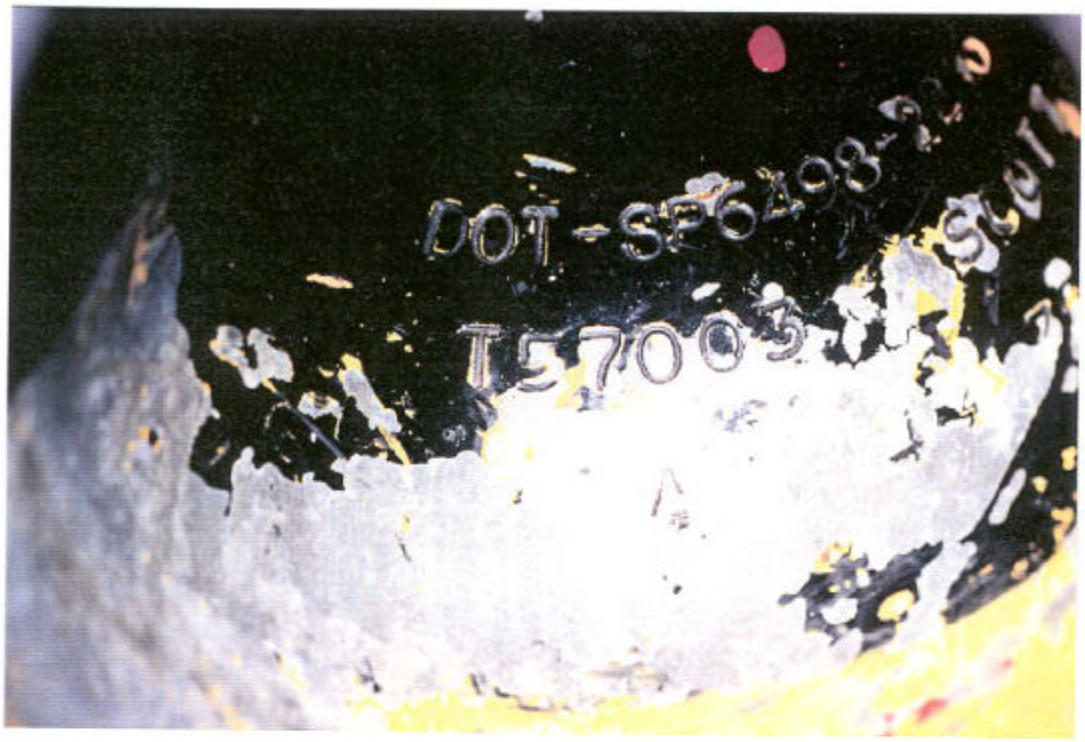

Photo ID: DC18128-R2E18

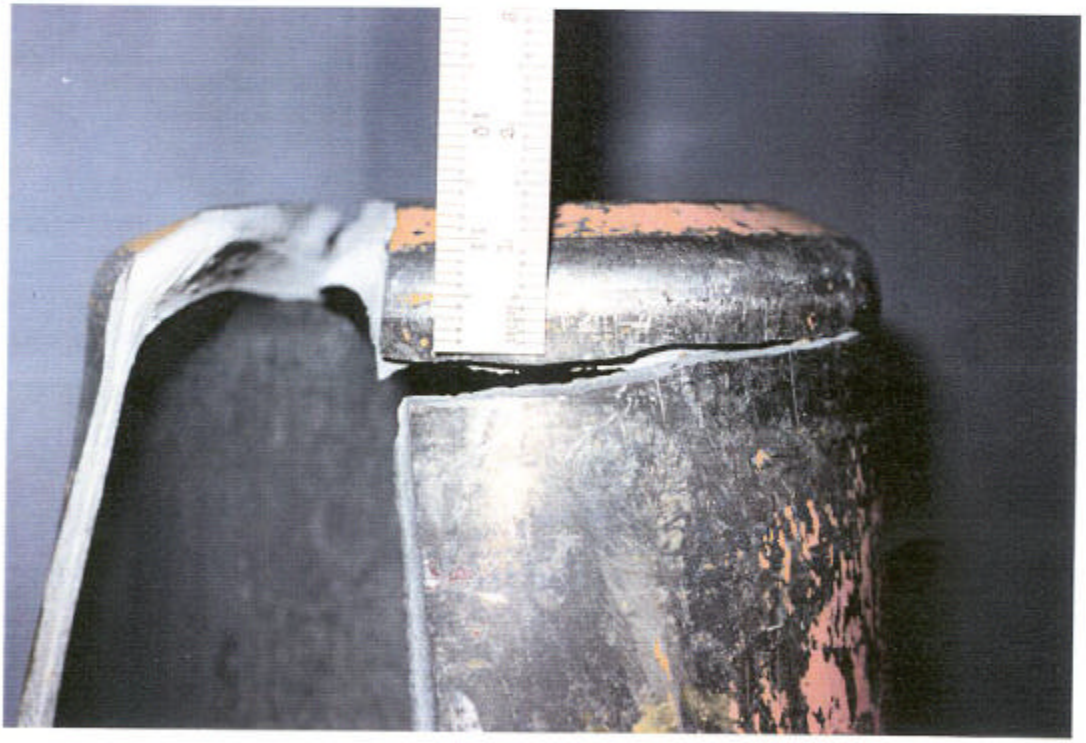

Photo ID: DC18128-R2E19

Ex.

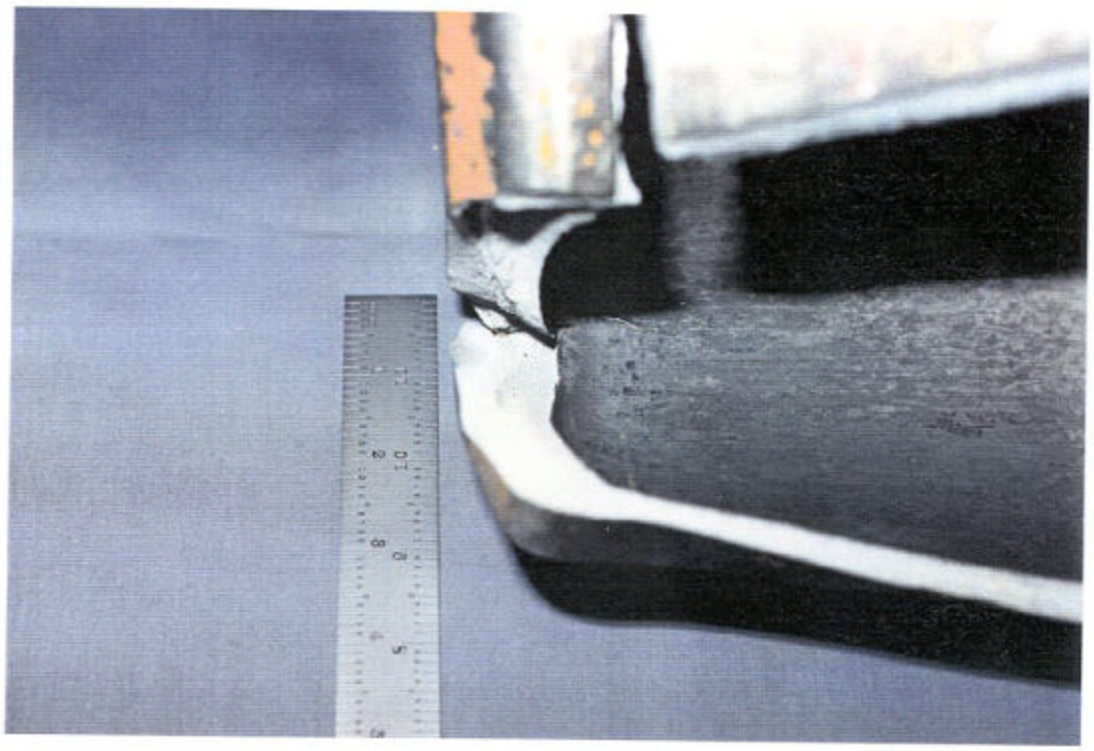

Photo ID: DC18128-R2E20

Photo ID: DC18128-R2E21

Photo ID: DC18128-R2E22

Photo ID: DC18128-R2E23

Photo ID: DC18128-R2E24

Photo ID: DC18128-R2E25